



Calhoun: The NPS Institutional Archive
DSpace Repository

Theses and Dissertations

1. Thesis and Dissertation Collection, all items

1990-06

Multiple channel satellite analysis of cirrus

Wieman, Sharon A.

Monterey, California: Naval Postgraduate School

<http://hdl.handle.net/10945/34837>

This publication is a work of the U.S. Government as defined in Title 17, United States Code, Section 101. Copyright protection is not available for this work in the United States.

Downloaded from NPS Archive: Calhoun



Calhoun is the Naval Postgraduate School's public access digital repository for research materials and institutional publications created by the NPS community. Calhoun is named for Professor of Mathematics Guy K. Calhoun, NPS's first appointed -- and published -- scholarly author.

Dudley Knox Library / Naval Postgraduate School
411 Dyer Road / 1 University Circle
Monterey, California USA 93943

<http://www.nps.edu/library>

AD-A238 054



2

NAVAL POSTGRADUATE SCHOOL

Monterey, California



DTIC
ELECTE
JUL 12 1991
S B D

THESIS

MULTIPLE CHANNEL SATELLITE
ANALYSIS OF CIRRUS

by

Sharon A. Wieman

June 1990

Thesis Advisor:

Carlyle H. Wash

Approved for public release; distribution is unlimited.

91-04495



91 7 09 069

Unclassified

SECURITY CLASSIFICATION OF THIS PAGE

REPORT DOCUMENTATION PAGE				Form Approved OMB No 0704-0188	
1a REPORT SECURITY CLASSIFICATION Unclassified			1b RESTRICTIVE MARKINGS		
2a SECURITY CLASSIFICATION AUTHORITY			3 DISTRIBUTION / AVAILABILITY OF REPORT Approved for public release; distribution is unlimited.		
2b DECLASSIFICATION / DOWNGRADING SCHEDULE					
4 PERFORMING ORGANIZATION REPORT NUMBER(S)			5 MONITORING ORGANIZATION REPORT NUMBER(S)		
6a NAME OF PERFORMING ORGANIZATION Naval Postgraduate School		6b OFFICE SYMBOL (If applicable) 35	7a. NAME OF MONITORING ORGANIZATION Naval Postgraduate School		
6c. ADDRESS (City, State, and ZIP Code) Monterey, CA 93943-5000			7b ADDRESS (City, State, and ZIP Code) Monterey, CA 93943-5000		
8a. NAME OF FUNDING / SPONSORING ORGANIZATION		8b OFFICE SYMBOL (If applicable)	9 PROCUREMENT INSTRUMENT IDENTIFICATION NUMBER		
8c. ADDRESS (City, State, and ZIP Code)			10 SOURCE OF FUNDING NUMBERS		
			PROGRAM ELEMENT NO	PROJECT NO	TASK NO
					WORK UNIT ACCESSION NO
11 TITLE (Include Security Classification) MULTIPLE CHANNEL SATELLITE ANALYSIS OF CIRRUS					
12 PERSONAL AUTHOR(S) Sharon A. Wieman					
13a TYPE OF REPORT Master's Thesis		13b TIME COVERED FROM _____ TO _____	14 DATE OF REPORT (Year, Month, Day) June 1990		15 PAGE COUNT 60
16 SUPPLEMENTARY NOTATION The views expressed in this thesis are those of the author and do not reflect the official policy or position of the Department of Defense or the U.S. Government.					
17 COSATI CODES			18 SUBJECT TERMS (Continue on reverse if necessary and identify by block number)		
FIELD	GROUP	SUB-GROUP	Meteorology, Satellite Remote Sensing, Cirrus, Split-Window Technique		
19 ABSTRACT (Continue on reverse if necessary and identify by block number) The split-window technique is based on the varying radiative properties of clouds and the atmosphere in different wavelengths of the primary infrared (IR) window. Channels 4 (11 micron) and 5 (12 micron) on the NOAA AVHRR are used to apply the technique to determine the differences between thick and thin cirrus and multiple layered clouds. The brightness temperature from channel 5 was subtracted from the brightness temperature from channel 4, resulting in a brightness temperature difference (BTD) image. The technique was applied to ten subscenes over mid-latitude land areas for both summer and winter cases. The BTD values were compared to surface observations of the same time period as the images. The cases were grouped into five and then three cloud groups based on the surface observations. The analysis of variance showed that the average BTD values for the three cloud groups were statistically different for the summer cases but not for the winter cases. The BTD thresholds estimated from these cases are: (1) Multiple layered clouds--0.00 to 0.80; (2) Thick cirrus--0.81 to 1.50 and (3) Thin cirrus--1.51 and greater. The split-window technique is					
20 DISTRIBUTION / AVAILABILITY OF ABSTRACT <input type="checkbox"/> UNCLASSIFIED/UNLIMITED <input type="checkbox"/> SAME AS RPT <input type="checkbox"/> DTIC USERS			21 ABSTRACT SECURITY CLASSIFICATION Unclassified		
22a NAME OF RESPONSIBLE INDIVIDUAL Carlyle H. Wash			22b TELEPHONE (Include Area Code) (408) 646-2295		22c OFFICE SYMBOL MR/WX

Unclassified

SECURITY CLASSIFICATION OF THIS PAGE

successful in distinguishing the varying cirrus thicknesses when the surface temperature is warmer than 285 K.

Approved for public release; distribution is unlimited.

Multiple Channel Satellite
Analysis of Cirrus

by

Sharon A. Wieman
Captain, United States Air Force
B.A., Gustavus Adolphus College, 1977

Submitted in partial fulfillment
of the requirements for the degree of

MASTER OF SCIENCE IN METEOROLOGY

from the

NAVAL POSTGRADUATE SCHOOL
June 1990

Author:

Sharon A. Wieman

Approved by:

Carlyle H. Wash, Thesis Advisor

Philip A. Durkee, Second Reader

Robert J. Renard, Chairman
Department of Meteorology

ABSTRACT

The split-window technique is based on the varying radiative properties of clouds and the atmosphere in different wavelengths of the primary infrared (IR) window. Channels 4 (11 micron) and 5 (12 micron) on the NOAA AVHRR are used to apply the technique to determine the differences between thick and thin cirrus and multiple layered clouds. The brightness temperature from channel 5 was subtracted from the brightness temperature from channel 4, resulting in a brightness temperature difference (BTD) image. The technique was applied to ten subscenes over mid-latitude land areas for both summer and winter cases. The BTD values were compared to surface observations of the same time period as the images. The cases were grouped into five and then three cloud groups based on the surface observations. The analysis of variance showed that the average BTD values for the three cloud groups were statistically different for the summer cases but not for the winter cases. The BTD thresholds estimated from these cases are: (1) Multiple layered clouds--0.00 to 0.80; (2) Thick cirrus--0.81 to 1.50 and (3) Thin cirrus--1.51 and greater. The split-window technique is successful in distinguishing the varying cirrus thicknesses when the surface temperature is warmer than 285 K.

TABLE OF CONTENTS

I.	INTRODUCTION	1
II.	THEORETICAL BACKGROUND	4
	A. MULTISPECTRAL STUDIES	4
	B. VARIATION IN CIRRUS RADIATIVE PROPERTIES WITH WAVELENGTH IN THE 10 - 12 MICRON WINDOW.	5
	C. SPLIT-WINDOW TECHNIQUE	6
III.	PROCEDURES	12
IV.	DATA ANALYSIS	16
	A. WINTER CASE	16
	B. SUMMER CASE	21
	C. JET CONDENSATION TRAILS CASE	27
V.	RESULTS	32
VI.	CONCLUSIONS	44
	LIST OF REFERENCES	47
	INITIAL DISTRIBUTION LIST	49

Accession For	
NTIS GRA&I	<input checked="" type="checkbox"/>
DTIC TAB	<input type="checkbox"/>
Unannounced	<input type="checkbox"/>
Justification	
By	
Distribution/	
Availability Codes	
Dist	Avail and/or Special
A-1	



LIST OF TABLES

Table 1.	CHANNEL 4-5 DIFFERENCE STATISTICS FOR FIVE CLOUD GROUPS--SUMMER CASES.	32
Table 2.	CHANNEL 4-5 DIFFERENCE STATISTICS FOR THREE CLOUD GROUPS--SUMMER CASES.	34
Table 3.	ANALYSIS OF VARIANCE FOR THREE CLOUD GROUPS--SUMMER CASES.	37
Table 4.	TUKEY'S TEST RESULT FOR THREE CLOUD GROUPS--SUMMER CASES.	38
Table 5.	T TEST FOR GROUPS 2 AND 3--SUMMER CASES.	39
Table 6.	CHANNEL 4-5 DIFFERENCES STATISTICS FOR FIVE CLOUD GROUPS--WINTER CASES.	39
Table 7.	STATISTICS FOR THREE CLOUD GROUPS--WINTER CASES	41
Table 8.	ANALYSIS OF VARIANCE FOR THREE CLOUD GROUPS--WINTER CASES.	41
Table 9.	BTD THRESHOLDS.	43

LIST OF FIGURES

Fig. 1. Brightness temperature difference as a function of emissivity	8
Fig. 2. Schematic two-dimensional diagram for cloud type classification	9
Fig. 3. 2307 UTC 16 Jan 88 subscene. Channel 2 image	17
Fig. 4. Same as Fig. 3 except channel 4 IR image	18
Fig. 5. Brightness temperature difference image for subscene in Fig. 3.	19
Fig. 6. Surface observations at 2300 UTC 16 January 1988	20
Fig. 7. 2234 UTC 28 June 1987 subscene. Channel 2 image	22
Fig. 8. Same as Fig. 7 except channel 4 IR image	23
Fig. 9. Brightness temperature difference image for same subscene in Fig. 7.	24
Fig. 10. Surface observations at 2200 UTC 28 June 1987	25
Fig. 11. Same as Fig. 10 except at 2300 UTC 28 June 1987.	26
Fig. 12. 2256 UTC 17 January 1988 subscene. Channel 2 image	28
Fig. 13. Same as Fig. 12 except channel 4 IR image	29
Fig. 14. Brightness temperature difference image for subscene in Fig. 12.	30
Fig. 15. Surface observations at 2300 UTC 17 January 1988	31
Fig. 16. Box plot of BTD data from the summer season--five cloud groups	33
Fig. 17. Box plot of BTD data from the summer season--three cloud groups	35
Fig. 18. Box plot of BTD data from the winter season--five cloud groups	40
Fig. 19. Box plot of BTD data from the winter season--three cloud groups	42

ACKNOWLEDGMENTS

I would like to thank Professor Carlyle Wash for his direction and guidance of my research. Mr. Craig Motell of the Naval Postgraduate School Meteorology Department provided immeasurable help with his expertise with the computer system and wrote several programs for my use. I also thank Professor Philip Durkee for his review of the thesis and advice on the research. I dedicate this work to my parents, Earl and Janet, who taught me the importance of doing a good job, and to my fiance, Keith, who provided support and encouragement.

I. INTRODUCTION

Knowledge of weather conditions is crucial to most military and civilian operations. Cloud cover is a particular weather element that may severely limit aerial and satellite reconnaissance missions, and flight and refueling operations. Cloud cover can be determined from surface observations; however, large gaps exist between surface stations, even over land areas. Meteorological satellite imagery analysis of cloud properties is vital to cover these areas. Satellite cloud analysis is a critical element of weather analysis and of understanding the physical processes of weather systems.

The identification of cirrus clouds often present difficulties during both operational and research analyses of satellite imagery. Due to the varying thickness of cirrus, accurate analysis of these ice crystal clouds is difficult. Thin cirrus clouds are very often semi-transparent in visible imagery and the terrain may be seen through the cloud. When using infrared (IR) wavelengths, contamination may result due to warmer radiance from lower levels penetrating through the thin cirrus clouds, making the clouds appear darker and lower than they actually are. (Anderson, *et. al.* 1969 and others)

Thicker cirrus, such as cirrostratus, appears cold (white) in the IR and reflective (also white) in the visual imagery. It is very difficult to differentiate between a single layer of cirrostratus and cirrostratus associated with lower cloud layers. If only one

IR channel is available, dense cirrus cloud may be misinterpreted as multiple layered clouds of a major storm system.

Several studies (Inoue 1985, Inoue 1987, Prabhakara, *et. al.* 1988 and Lee 1989) have shown that the split-window technique, which uses channels 4 (10.3 - 11.3 micron) and 5 (11.5 - 12.5 micron) on the National Oceanic and Atmospheric Administration (NOAA) satellite's Advanced Very High Resolution Radiometer (AVHRR), can be used to improve the satellite analysis of cirrus. This technique involves subtracting the brightness temperatures on channel 5 from the brightness temperatures on channel 4 and displaying the results as a brightness temperature difference image. Results have shown that the varying thicknesses of cirrus can be distinguished using this technique over the tropical oceans.

The objective of this thesis is to study the use of the split-window technique in mapping cirrus in the mid-latitudes. The split-window technique will be applied to a variety of cases to determine the split-window differences for thick and thin cirrus, and for multiple layer clouds. Visual and IR satellite images, as well as the brightness temperature difference images, will be compared with surface observations to determine areas of cirrus. All of the cases will be over land to facilitate the evaluation of cirrus with ground truth data. Both summer and winter seasons will be investigated. The ultimate goal is to estimate seasonal thresholds to improve the objective cloud analysis of cirrus.

In Chapter II the key papers describing the varying radiative properties of cirrus and the split-window technique are reviewed. Chapter III describes the procedures

that are used in this cloud research. The data analysis is given in Chapter IV. The results and conclusions follow in Chapters V and VI.

II. THEORETICAL BACKGROUND

A. MULTISPECTRAL STUDIES

Researchers have applied various multispectral methods to analyze cirrus. In an early study, Reynolds, *et. al.* (1978) applied a subtraction method to visible and IR Geostationary Operational Environmental Satellite (GOES) imagery to discriminate different cloud types. During this subtraction method or spectral differencing, the raw IR and visual counts for each pixel were normalized to an 8-bit scale (0-255 gray shades). The visible counts were subtracted from the infrared counts. The difference values were compared with surface observations. They found that the high difference values corresponded to cirrus clouds and the low difference values corresponded well with low clouds or snow cover. The middle range of values corresponded with deeper clouds associated with the precipitation region of the storm system studied. Obvious cloud type signatures appeared while using this approach. The technique was especially useful to separate snow from clouds and to identify cirrus.

Platt (1983) also used a bispectral approach with a physical cloud model to determine cloud amount and optical depth and to show the effects of variable solar zenith angle and satellite viewing angle on satellite radiances. He derived bispectral curves of visible albedo versus infrared brightness temperature for idealized cloud

layers. The layers varied between the overcast case with variable optical depth (like cirrus clouds) to cases with a uniform high optical depth but with variable cloud cover as with stratocumulus. The theoretical curves were compared with observational data obtained from the Japanese Geostationary Meteorological Satellite (GMS). The various cloud types from the theoretical curves matched well with the same type of clouds from the observational data.

B. VARIATION IN CIRRUS RADIATIVE PROPERTIES WITH WAVELENGTH IN THE 10 - 12 MICRON WINDOW.

Liou (1974) solved the radiative transfer equation for moist and dry model cloudy atmospheres to derive the emission, transmission and reflection properties of cirrus clouds. He was specifically interested in the properties in the 8 - 12 micron window region because absorption due to the atmospheric gases is relatively small there.

The phase function, extinction cross section and single scattering albedo were derived at various wavelengths for the different characteristics of cloud particles. These cloud characteristics are the shapes, sizes and orientations of cloud particles and the associated real and imaginary parts of the refractive indices. By using data from Irvine and Pollack (1968), Liou found that the imaginary part of the refractive index for ice is larger in the 11.5 - 12 micron region than in the 8 - 11 micron region. The imaginary part of the refractive index determines the absorption properties of

the ice particles. Liou concluded that cirrus clouds have greater absorption in the longer wavelength region.

Hunt (1973) also used the data from Irvine and Pollack (1968) to derive the radiative properties of ice crystals. Radiative properties are a function of wavelength. As the wavelength increases in the thermal window, the emissivity and reflectivity of cirrus increase and the transmissivity decreases.

Both of these studies show that absorption is greater in the longer wavelengths of the primary IR window region. A cloud that is a good absorber is a good emitter. Greater emissivity and reflectivity lead to decreased transmissivity, resulting in colder brightness temperatures being observed at the longer wavelengths of the thermal IR window.

C. SPLIT-WINDOW TECHNIQUE

Inoue (1985) used channels 4 (11 micron) and 5 (12 micron) on the NOAA AVHRR to retrieve cloud top temperature and effective emissivity for semi-transparent cirrus clouds. Both of these channels are in the primary IR window region, resulting in the method being referred to as "split-window". He found the brightness temperature is warmer in channel 4 and the effective emissivity is greater in channel 5 in agreement with earlier studies of Liou (1974) and Hunt (1973).

Inoue's original AVHRR data were converted to 8-bit data with 0.5 K temperature resolution. The brightness temperature from channel 5 was subtracted from the brightness temperature from channel 4 to form a difference image. The

lighter area of the difference image referred to the larger temperature difference between the two channels while the darker area referred to the smaller temperature difference. A visible image from channel 1 (0.58 - 0.68 micron) and a channel 4 image of the same area were compared with the difference image. Semi-transparent cirrus corresponded to the larger temperature difference (light area) while cumulonimbus or thick cirrus clouds corresponded well to the smaller temperature difference (dark area). Cirrus clouds were easily identified from the brightness temperature difference image, illustrating that the two channels have different radiative properties for cirrus clouds in this wavelength region, as Liou (1974) indicated.

In a later study, Inoue (1987) used cloudy and cloud-free areas to empirically determine a relationship between the emissivities of channels 4 and 5 as

$$\epsilon_5 = 1 - (1 - \epsilon_4)^{1.08}, \quad (1)$$

where ϵ_4 and ϵ_5 are the emissivity for channels 4 and 5, respectively. He plotted the brightness temperature difference ($T_4 - T_5$) of channels 4 and 5 as a function of emissivity in channel 4 (Fig. 1). Generally, the brightness temperature difference (BTD) is positive and a negative value is considered to be noise. Zero emissivity corresponds to a cloud-free area while emissivity of 1.0 corresponds to thick cirrostratus or cirrus on top of cumulonimbus. Semi-transparent cirrus is characterized as cloud with emissivities between zero and 1.0 and possessing a larger BTD than that of cloud-free areas. Fig. 1 suggests that brightness temperature

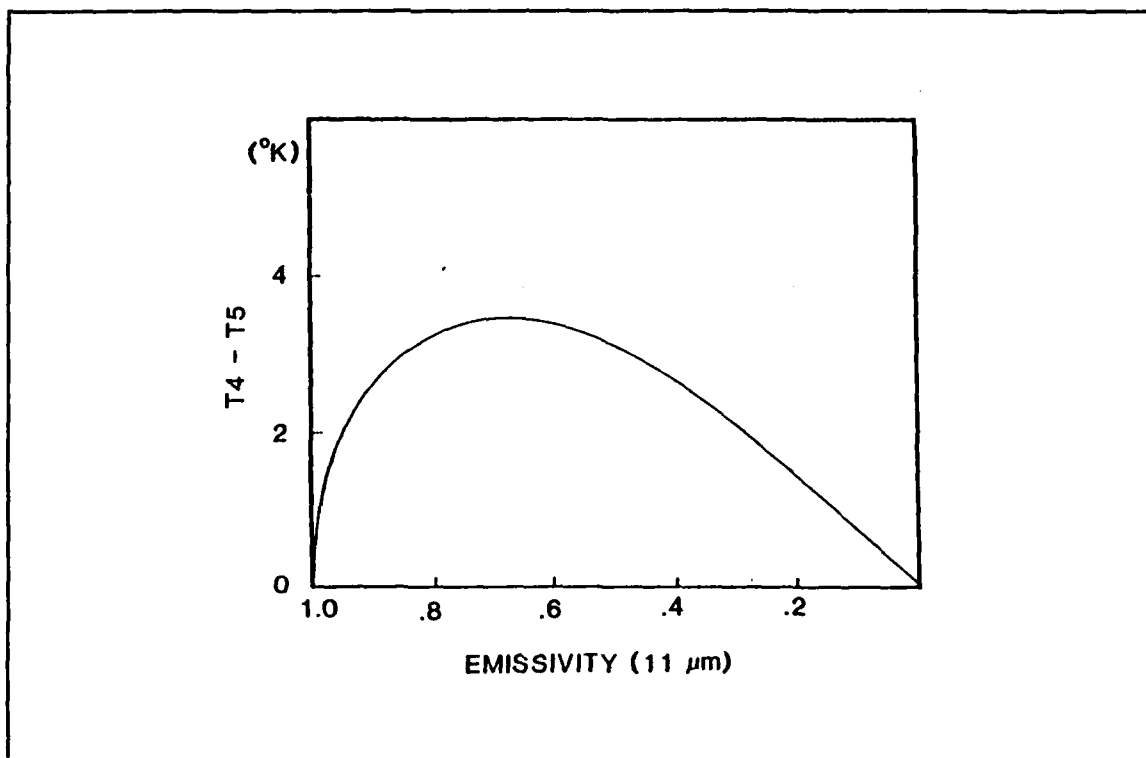


Fig. 1. Brightness temperature difference ($T_4 - T_5$) as a function of emissivity in channel 4. The curve is for mid-latitude cirrus with temperature near 210 K and a surface near 285 K. After Inoue (1987).

differences greater than 1 to 2 K can be used to identify thin cirrus. Other cloud types and cloud-free atmosphere have smaller differences. (Lee 1989)

Inoue then applied the split-window method to determine thresholds for the various cloud types by plotting the channel 4 brightness temperature versus the BTd. A schematic two-dimensional diagram for cloud type classification was created to distinguish between cirrus, dense cirrus, cumulonimbus and cumulus clouds (Fig. 2). The axes of the diagram were the brightness temperature of channel 4 and the brightness temperature difference between channels 4 and 5. Inoue referred to cirrus as cirriform cloud, dense cirrus means cirriform clouds with emissivity greater than

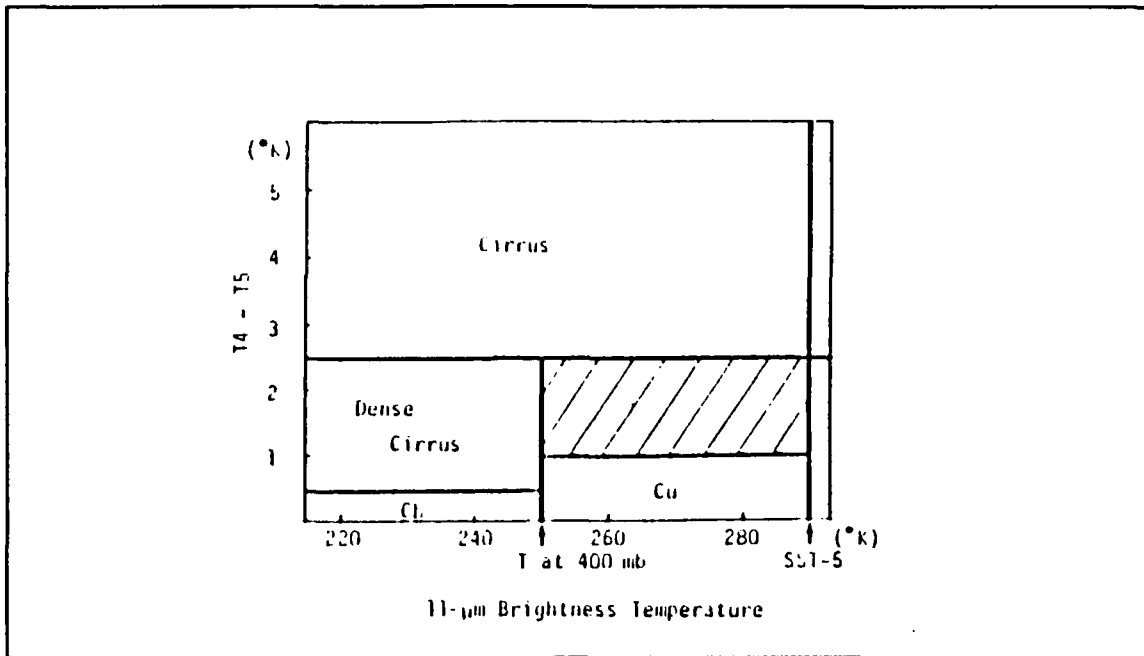


Fig. 2. Schematic two-dimensional diagram for cloud type classification. After Inoue (1987).

about 0.8 and cumulus means cumuliform clouds including stratocumulus. The hatched area in Fig. 2 is nonclassified clouds, characterized as low-level cloud overlaid by very thin cirrus, thin low-level cloud or low-level overcast cloud which partially fills the field of view of the instrument.

Inoue used the climatological 400 mb temperature as the threshold for high-level and low-level cloud classification (Fig. 2). The maximum channel 4 brightness temperature (labeled sea-surface temperature (SST) minus 5 K in Fig. 2) is used as the cloud/no cloud threshold.

Inoue restricted his studies to data over the tropical ocean because both the temperature and emissivity of land can vary rapidly with time and space. Attempts to distinguish between cumulus and cirrus cloud become more difficult in higher

latitudes because the BTD over cloud-free areas is small due to the lower upwelled radiances from the colder surface temperature. Also, the BTD is 2 K larger over tropical oceans than over mid-latitude land due to the differential water vapor attenuation in the two bands. (Inoue 1987)

Cirrus and cumulus clouds were generally well classified with this method, except for very thin cirrus and low-level cloud overlaid by very thin cirrus. These results were supported by inspection of visible and infrared images compared to nephanalysis charts analyzed from GMS image data at the Japan Meteorological Satellite Center (JMSC).

In another recent AVHRR study, Lee (1989) used the split-window technique to identify jet condensation trails (contrails). Since the contrails consist of thin cirrus, the contrail appears 2 to 5 K warmer in channel 4 than in channel 5. However, the BTD values of contrails varied from scene to scene making it impossible to determine precise thresholds for contrail detection.

Prabhakara, *et. al.* (1988) applied the split-window technique to Nimbus-4 IR data at two wavelength bands at 10.8 and 12.6 micron. They restricted their application to over ocean areas and constructed mean seasonal maps of the distribution of thin cirrus clouds over the oceans from 50°N to 50°S. The areas of thin cirrus determined by maximum temperature differences of 8 K and greater matched well with the convectively active areas such as the Inter-Tropical Convergence Zone (ITCZ), South Pacific Convergence Zone (SPCZ) and the Bay of Bengal.

These studies reveal that the varying radiative properties of ice in the primary IR window region can be applied to the determination of areas of thick and thin cirrus, and multiple layer clouds. This thesis examines further the split-window cirrus analysis. Previous studies have been limited to cases over the tropical oceans. All cases in this study will be over the mid-latitudes and land areas so surface observations may be used for comparisons and to evaluate the use of this technique. Since operational cloud analysis uses both satellite and ground observer observations, it is important to compare surface cloud observations with split-window cirrus estimates. The cases examined are divided into the summer and winter seasons to estimate seasonal thresholds for the different thicknesses of cirrus.

III. PROCEDURES

Subscenes with areas of thick and thin cirrus and multiple layered clouds were chosen from overviews of NOAA AVHRR passes. The Naval Postgraduate School (NPS) Interactive Digital Environmental Analysis (IDEA) Laboratory was used to process the imagery. All channel data were measured with the AVHRR sensor on board the NOAA satellites. These data are in the form of 10-bit raw counts for each pixel. Channels 1 and 2 raw counts are converted to albedo using calibration coefficients obtained before the satellite was launched. Channels 3 through 5 raw counts are converted to radiances using calibration coefficients obtained onboard the NOAA satellites by the AVHRR sensor itself. These radiances are converted to brightness temperatures using the inverse Planck's equation. The radiometric resolution of the data is reduced from the original 10-bit to 8-bit for display purposes. The temperature resolution is approximately 0.5 K.

Ten subscenes were chosen for analysis. Five images were made for each subscene--channel 2 (0.72 - 1.10 micron) near IR reflectance, channels 4 and 5 brightness temperatures, brightness temperature difference (BTD) and an enhanced image of the brightness temperature difference.

The temperature difference image was prepared by subtracting the channel 5 brightness temperature from the corresponding channel 4 brightness temperature. These temperature differences are then displayed as an image. The original BTD

images lacked contrast because of the very small range of actual temperature differences. On most of the images, the brightness temperature differences ranged from 0 to 3 K. A mid-afternoon summer case located in northern California did have values that were much higher, reaching a maximum of 12.3 K. These extreme values were caused by the attenuation of atmospheric water vapor and will be explained in Chapter IV, Section B.

The BTD images were then enhanced with a Histogram Equalization Program. This Program is a general nonlinear transformation that tends to automatically reduce the contrast in very light or very dark areas (Schowengerdt 1983). It enhances the contrast for the most common gray shades of the histogram.

Hourly surface observations for the same time period as the satellite pass were obtained. If the satellite pass occurred in the middle of the hour, the observations from the preceding and following hours were both used. All stations that reported high-level clouds, mid- or low-level overcast cloud layers or precipitation were noted.

The stations of interest were then located on the subscene by use of a latitude and longitude grid that was computed through the navigation files on the satellite data tape. The stations' positions are accurate to within 5 km and this may introduce some error in the data. An averaging program was used to compute mean BTD values. A 7 x 7 pixel square area was used for this study. Each pixel is approximately 1 km near nadir. The region will cover a larger area if the station is away from nadir. This averaging will partly compensate for errors in locating the observing stations on the image and motion of the clouds that occurred between the

time of the surface observations and the time of the satellite pass. The gray shade for each pixel in the area is read and converted back to its original brightness temperature. The average brightness temperature and brightness temperature difference for the area is then computed along with its standard deviation.

The average brightness temperature differences were compared with all the reporting stations of interest. Because surface observations may contain different combinations of cloud layers, five cloud groups were created:

1. Predominantly high-level broken or overcast clouds, including thin overcast and thin broken.
2. Predominantly high-level scattered clouds, including thin scattered.
3. Predominantly high- and mid-level broken or overcast clouds.
4. Predominantly multiple layered clouds (high-, mid- and low-level broken or overcast).
5. Stations reporting precipitation.

Also, stations reporting mid- or low-level scattered clouds under a high-level cloud deck were included in group one above. Stations reporting mid- or low-level scattered clouds under a high scattered clouds were included in the second group. Stations reporting low-level scattered clouds under high- and mid-level broken or overcast clouds were included in group three.

Cloud top temperatures were checked for stations that reported a low- or mid-level overcast layer. If the cloud top temperature was as cold as other stations in the area reporting high-level clouds, then it was assumed there were high-level clouds over that station that could not be seen from the ground due to the overcast low- or

mid-level clouds. These stations were included in either category three or four, depending if there was a low-level cloud layer. These five data groups were further separated into the summer and winter groupings. BTD statistics were completed for each group and will be presented next.

IV. DATA ANALYSIS

Ten cases were analyzed with the procedures described in chapter III. Four of these cases occurred during the winter and six during the summer months. This chapter will describe one winter and one summer case plus an unusual case showing jet condensation trails. Statistics for all the cases follow in Chapter V.

A. WINTER CASE

The winter case is from a NOAA-9 pass at 2307 UTC 16 January 1988. The subscene selected is located in the region of eastern Nevada, Utah, the western two-thirds of Colorado and the extreme southern part of Wyoming. The channel 2 near IR image with a latitude and longitude grid is shown in Fig. 3 followed by the channel 4 IR image (Fig. 4). The channel 5 image (not shown) is very similar to the channel 4 image.

As evident in both the visible and IR images, cirrus clouds cover most of the subscene north of 38°N and west of 110°W . The cirrus clouds also extend south of 38°N in the subscene between 112° and 114°W . An area of very thick, textured clouds is located between 39° and 40°N and 114° and 116°W . The area on the southwest edge of the image appears clear on the visible image but a small area of thin cirrus can be seen on the IR image. Another major cloud area can be seen on

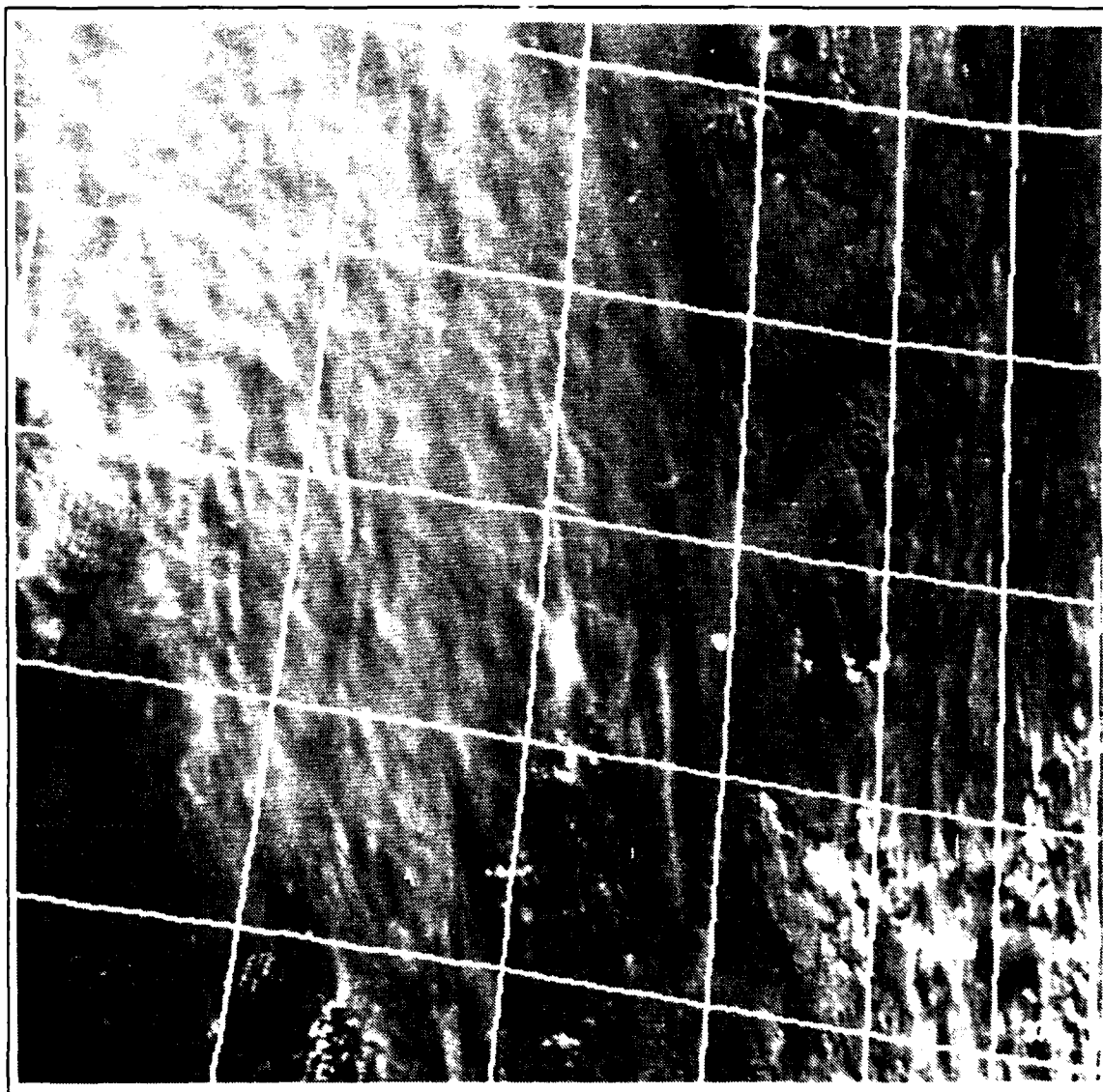


Fig. 3. 2307 UTC 16 Jan 88 subscene. NOAA-9 AVHRR channel 2 visible image with 1° latitude and 2° longitude grid.

the very eastern part of the image. Between these two areas are lower clouds over the Rocky Mountains.

The enhanced brightness temperature difference image for this subscene is shown in Fig. 5. The larger cloud mass covering the western half of the image is



Fig. 4. Same as Fig. 3 except channel 4 IR image without grid.

shown as varying shades of gray to bright white. The darker areas in this cloud mass correspond to smaller BTD values. Previous studies suggest these are regions of thick cirrus or multi-layered clouds. The bright white areas correspond to the larger BTD values and possibly regions of thin cirrus. The clear area to the southwest of this cloud mass is black on this difference image corresponding to a very small BTD



Fig. 5. Brightness temperature difference image for subscene in Fig. 3.

values. The colder cloud area in the extreme southwest corner of the IR image (Fig. 4) appears bright white in the BTD image, strongly suggesting this is thin cirrus. The cloud region on the eastern part of the image also shows varying shades of gray to white relating to regions of multi-layered clouds. The area of lower clouds over the

Rockies is darker in the BTD image than the areas of high clouds but not as dark as the clear area suggesting this is a region of low-level clouds.

Fig. 6 presents the surface observations for 2300 UTC 16 January 1988. The box on the figure illustrates the area of the subscene. The observations in the middle region of the large cloud mass indicate thick cirrus (mid- and high-level clouds).

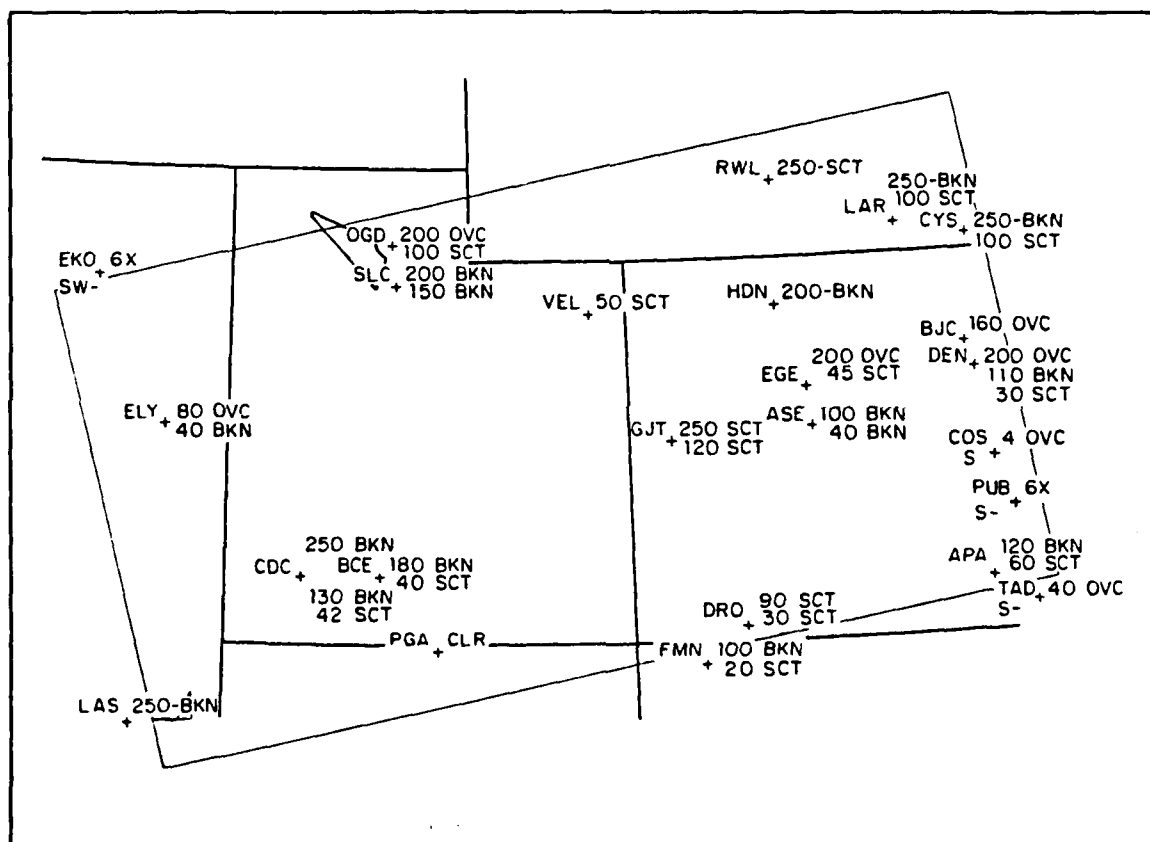


Fig. 6. Surface observations at 2300 UTC 16 January 1988 for the subscene in Fig. 3.

Scattered high-level clouds are reported along the edge of the cloud mass. Las Vegas, Nevada (LAS) is located on the southwest edge of the scene and is reporting 250 -BKN. This confirms the thin cirrus classification for this large BTD area. The

surface observations along the eastern edge of the area report multiple layered clouds and snow.

The brightness temperature difference image successfully highlights regions of thin cirrus for this case and agrees with subjective interpretation of the visual and IR images, and the surface observations.

B. SUMMER CASE

The summer case illustrated is from a NOAA-9 pass at 2234 UTC 28 June 1987. The subscene selected is centered over the northern half of California and extends into western Nevada and southern Oregon. The channel 2 near IR image with a latitude and longitude grid is shown in Fig. 7 followed by a channel 4 IR image (Fig. 8).

The California coastline is visible on the very western edges of the images. A large area of high clouds associated with large cumulonimbus cloud extends from the southeastern corner to the center of the image. A smaller thunderstorm is centered around 41°N , 121°W . A number of smaller cloud masses can be seen throughout an otherwise clear scene.

The clouds just offshore appear to be the same brightness in the visible image as the edge of the cumulonimbus but the IR image clearly shows that they are much warmer and lower. The low clouds mark the location of the San Francisco Bay on

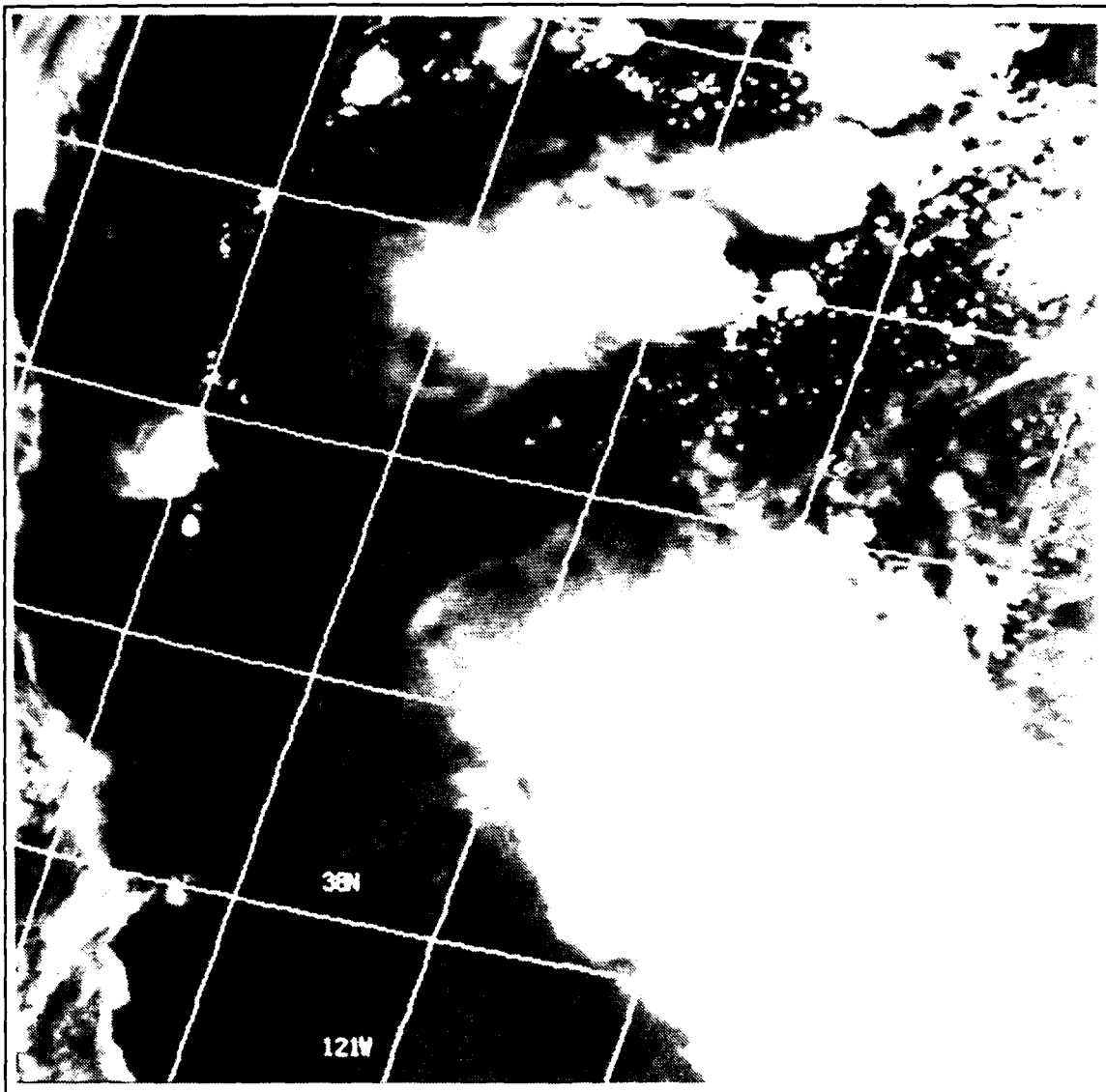


Fig. 7. 2234 UTC 28 June 1987 subscene. NOAA-9 AVHRR channel 2 visible image with 1° latitude and 1° longitude grid.

the visible image. The edges of the cumulonimbus appear to be thin cirrus on the visible but the rest of the cloud mass has the same bright reflectance, representing the cirrus and multiple layered clouds.

The enhanced brightness temperature difference image for this subscene is shown in Fig. 9. The cumulonimbus regions vary from a very dark shade in the

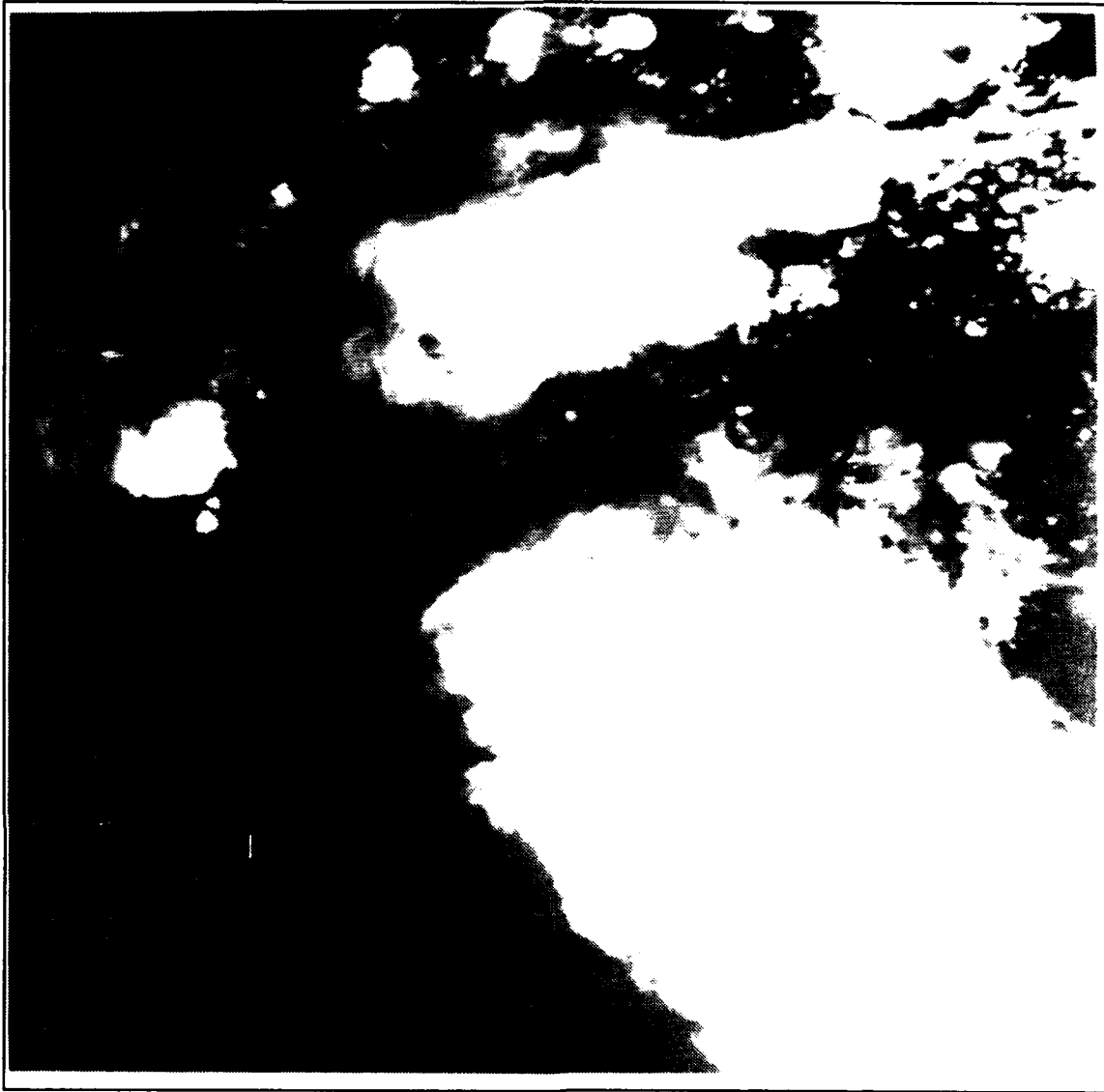


Fig. 8. Same as Fig. 7 except channel 4 IR image without grid.

center representing small BTD values and multi-layered clouds to a very bright white on the edges representing large BTD values and thin cirrus. The low, warm clouds over the ocean appear black due to the zero BTD value. The BTD values are non-zero over the clear California land areas as seen in the varying shades of gray. The atmospheric water vapor likely produces BTD values in this area. Inoue (1987)

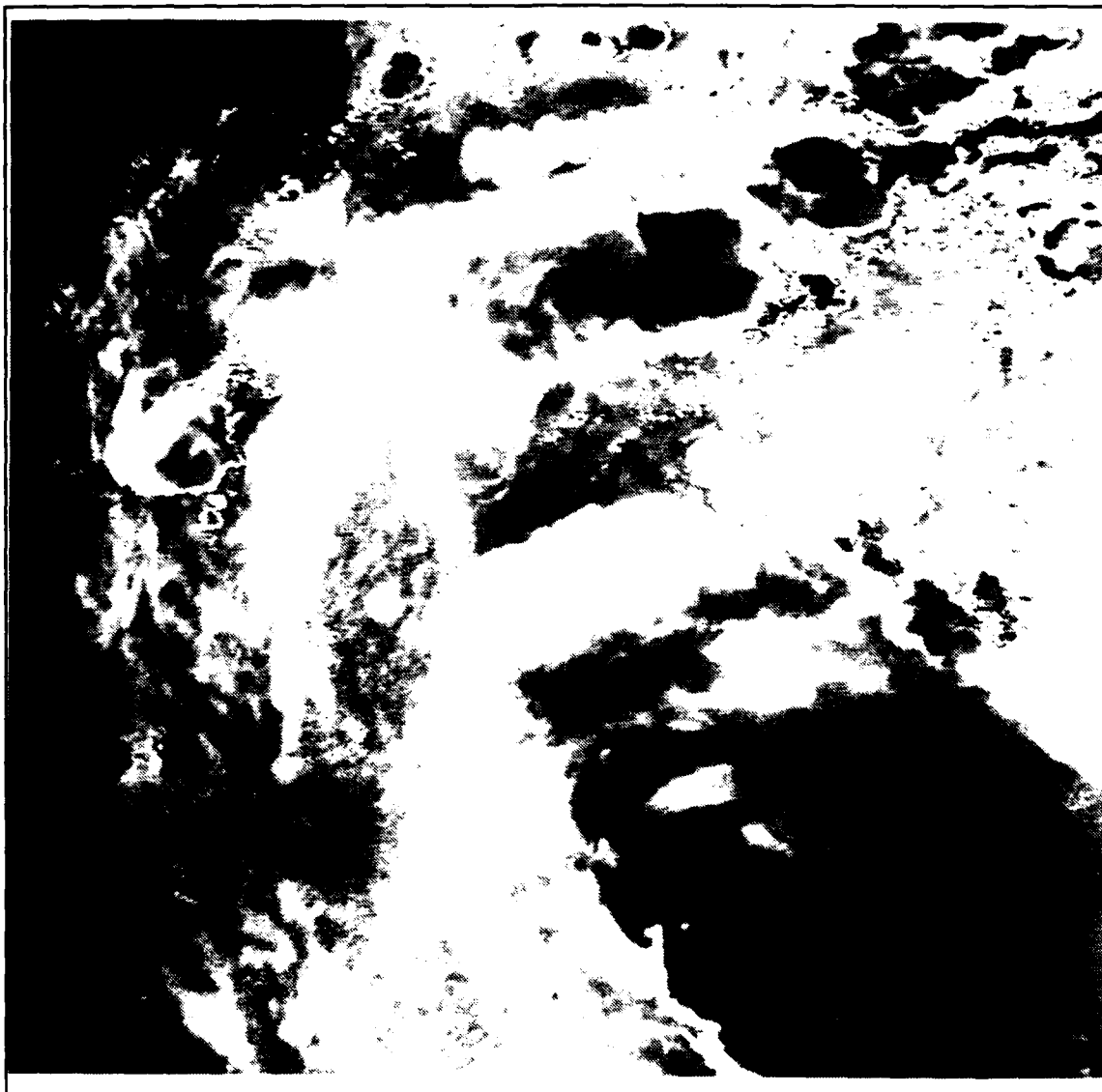


Fig. 9. Brightness temperature difference image for same subscene in Fig. 7.

found that the BT_D is 2 K larger over tropical oceans than over mid-latitude land due to the differential water vapor attenuation in the two bands.

Figs. 10 and 11 show the surface observations on 28 June 1987 at 2200 UTC and 2300 UTC respectively with the area of the subscene illustrated. Several stations are located under major dark area (low BT_D) in this scene. South Lake Tahoe,

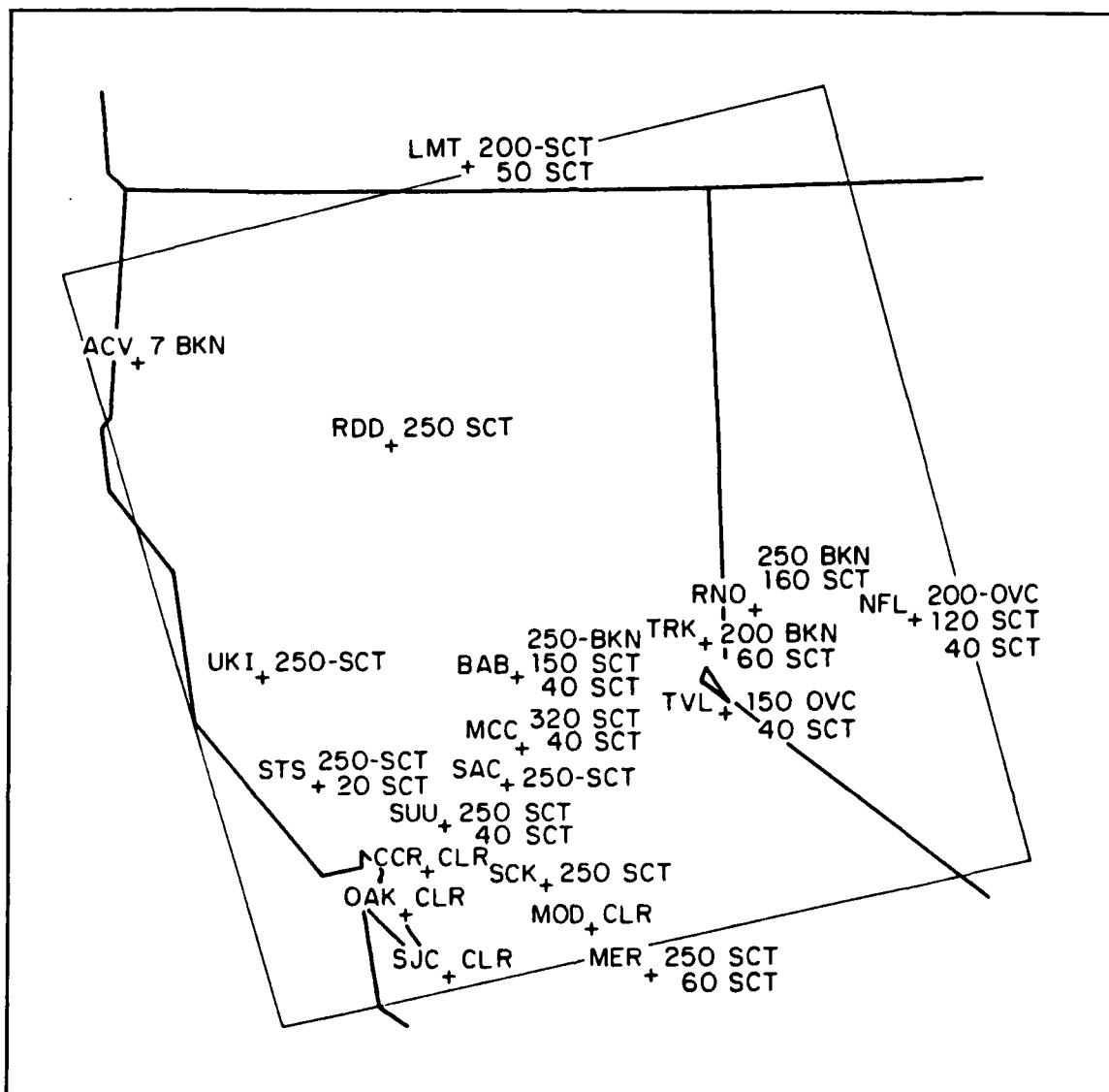


Fig. 10. Surface observations at 2200 UTC 28 June 1987 for subsense area in Fig. 7.

California (TVL) is reporting 150 OVC. A high-level cloud layer is likely present because there are very cold cloud top temperatures over this station. Fallon Naval Air Station, Nevada (NFL) is reporting multi-layered clouds for both time periods and thunderstorms at 2300 UTC. These reports confirm the analysis of multiple layered clouds and/or precipitation associated with the low BTD areas.

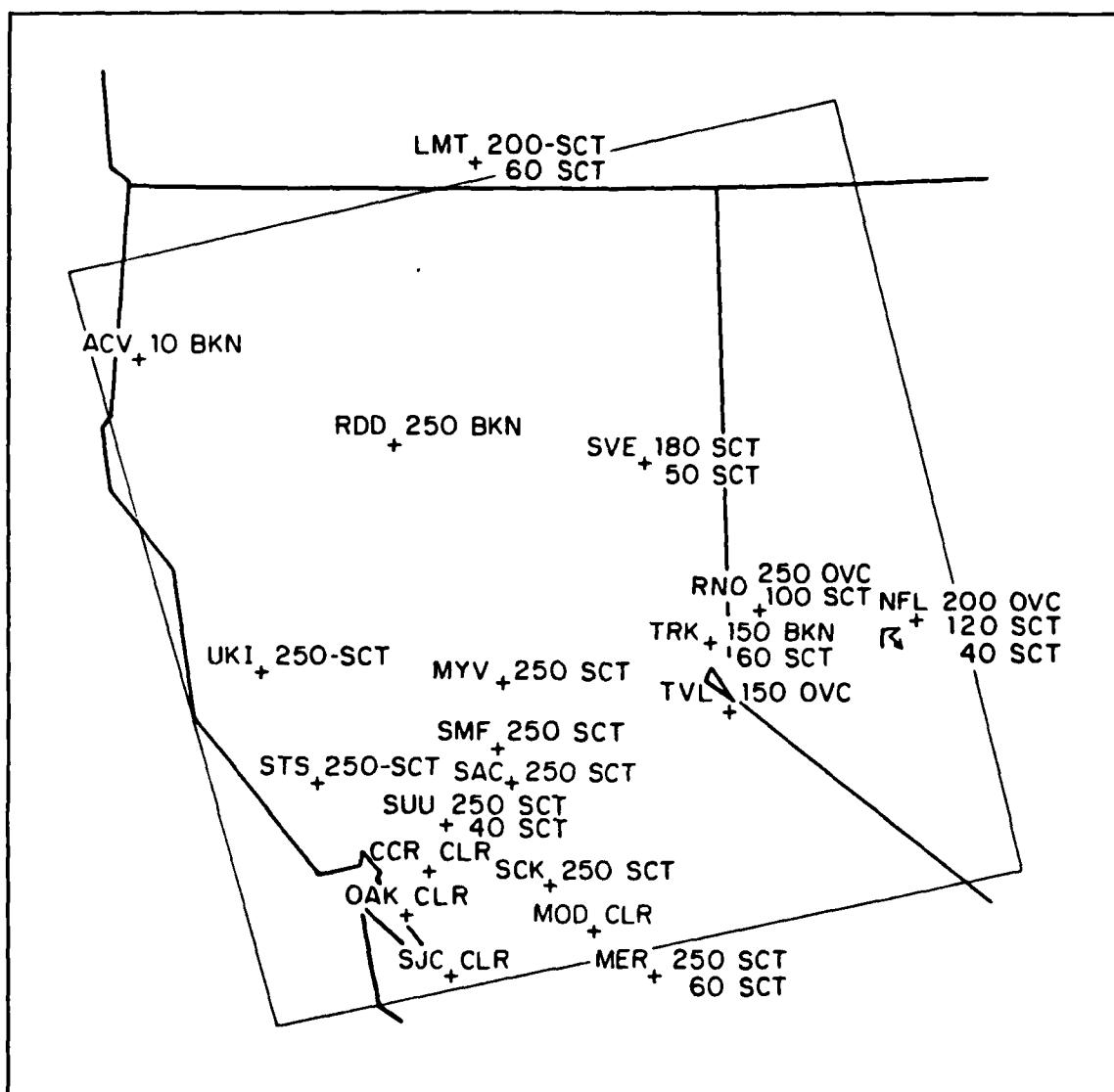


Fig. 11. Same as Fig. 10 except at 2300 UTC 28 June 1987.

High-level scattered clouds are reported around the perimeter of the large cumulonimbus in the region of very bright white on the brightness temperature difference image (large BTD values). Stations reporting thin cirrus in this area are Beale Air Force Base (BAB), Marysville (MYV), McClellan Air Force Base (MCC), Sacramento (SAC), Travis Air Force Base (SUU), and Stockton (SCK), all in

California. This example shows very clearly that this technique can delineate areas of thick and thin cirrus.

C. JET CONDENSATION TRAILS CASE

An unusual case was found in this study which indicates that the split-window technique can locate condensation trails (contrails) from jet aircraft. Contrails are elongated, tubular clouds of water and ice crystals frequently observed behind aircraft flying in clear and cold air. Contrails form as aircraft add water vapor and heat from the exhaust of combustion products from the engines. The effect is important only for rather low temperatures similar to those encountered near the tropopause (Huschke 1959). If the air is saturated, clouds probably already exist and the contrails will not be seen.

The subscene, from a NOAA-9 pass at 2256 UTC 17 January 1988, is located over Oregon, the northeastern corner of California and the northwestern corner of Nevada. The channel 2 near IR image with a latitude and longitude grid is shown in Fig. 12 followed by the channel 4 IR image (Fig. 13). Reporting stations are marked on this image by a 7 x 7 pixel square. This illustrates the area used by the threshold program to determine the average brightness temperature.

Some clear areas over the snow cover can be seen on the visible image. Areas of thin cirrus can be seen along the southern border of the visual image, in the northwestern corner of the subscene extending eastward along 43°N. The entire IR image lacks contrast due to the presence of the cold, snow-covered ground. The

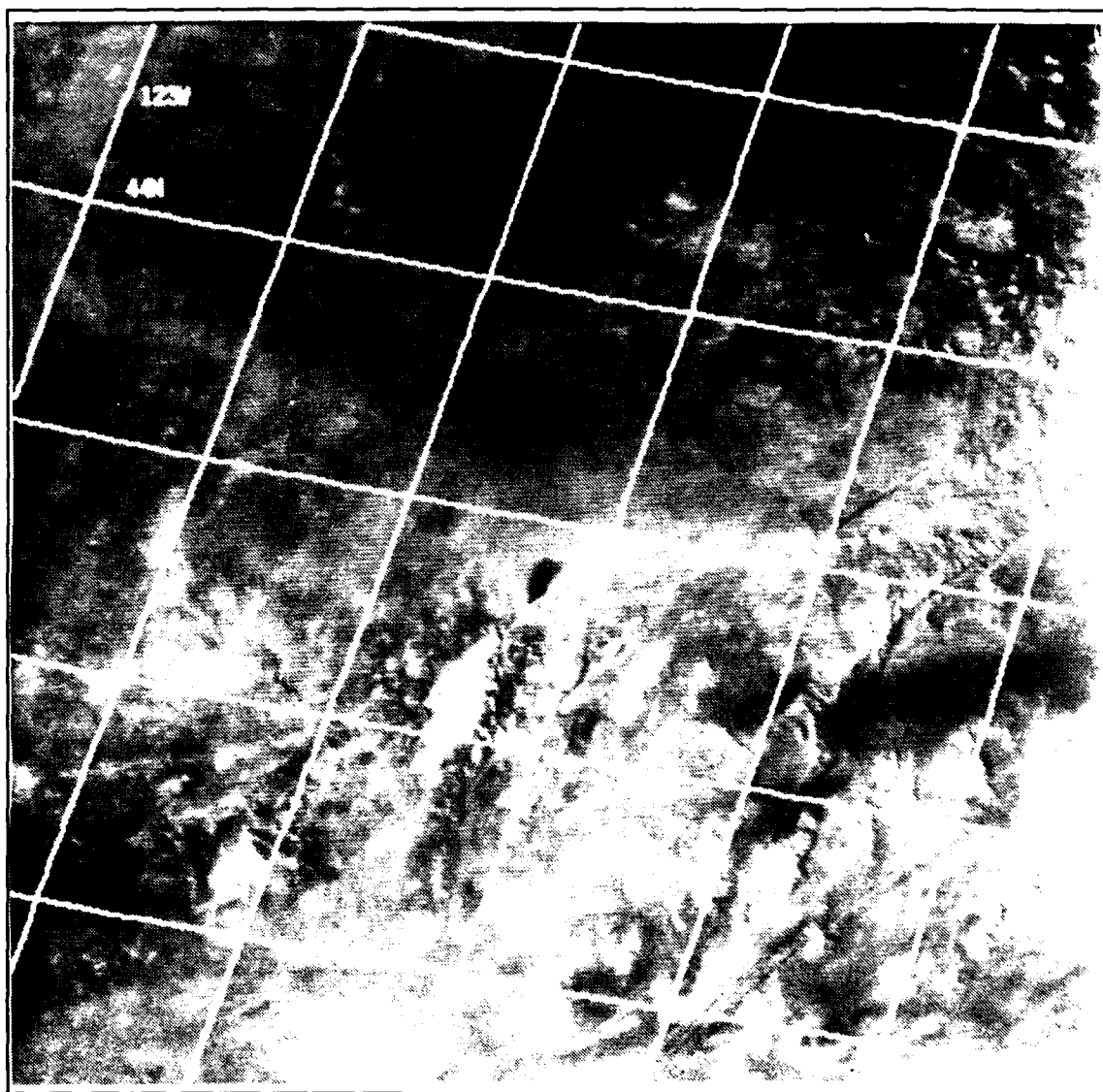


Fig. 12. 2256 UTC 17 January 1988 subscene. NOAA-9 AVHRR channel 2 visible image with 1° latitude and 1° longitude grid.

surface temperature is very close to the apparent cloud top temperature, resulting in the similar gray shades.

The enhanced brightness temperature difference image for this subscene is shown in Fig. 14. The areas of thin cirrus that were evident on the visual image appear as the very white areas representing large BTD values. The clear areas

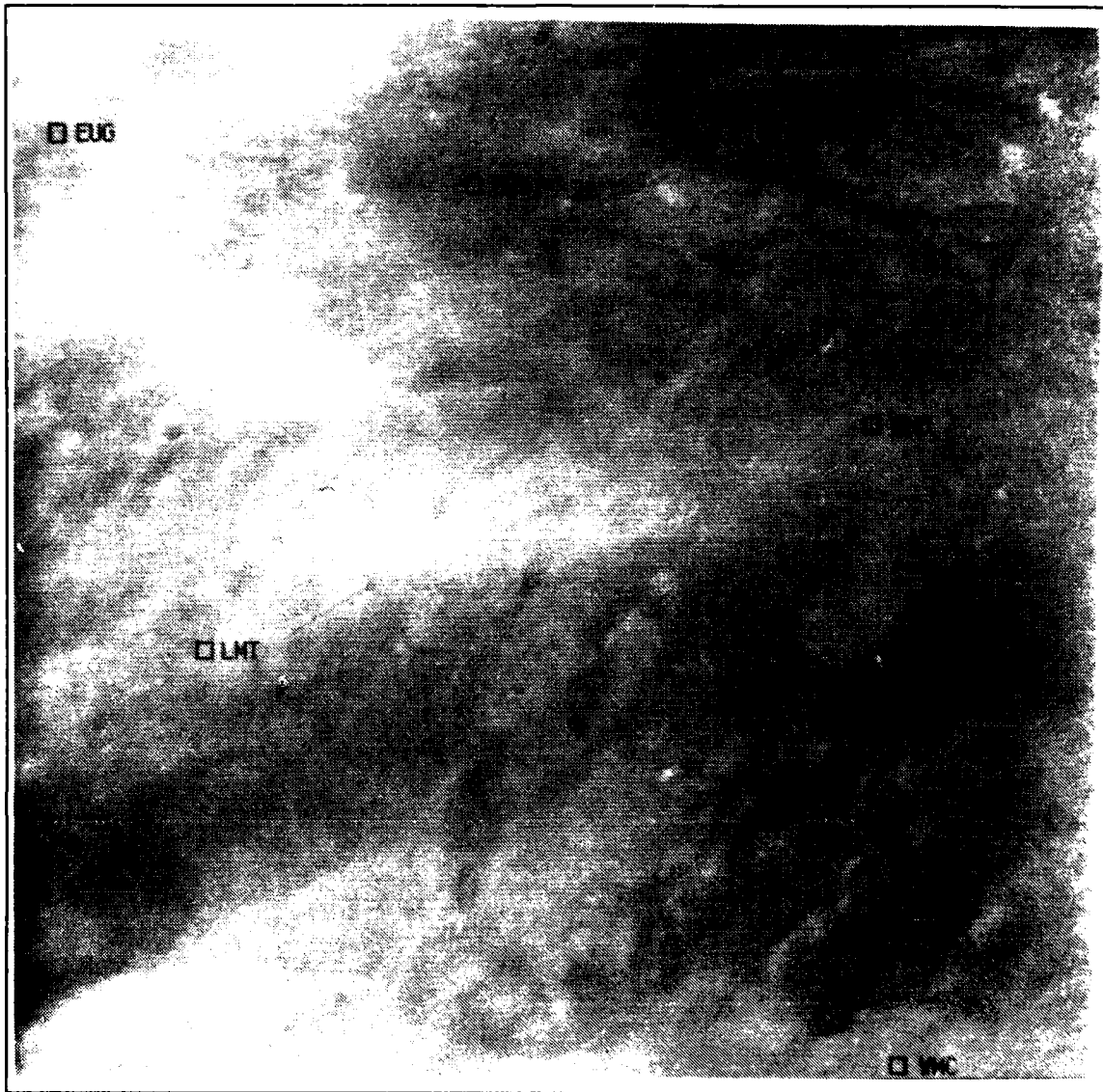


Fig. 13. Same as Fig. 12 except channel 4 IR image without grid. Reporting stations are marked with a 7 x 7 pixel area.

correspond to zero BTD values and are black. The surface observations from 2300 UTC 17 January 1988 are shown in Fig. 15. Observations of high-level clouds are reported in the areas of very bright white on the BTD image.

The very thin but distinct bright lines on the BTD image are not detected on either the visual or IR images. They have BTD values that range from 1.5 K to 3.0

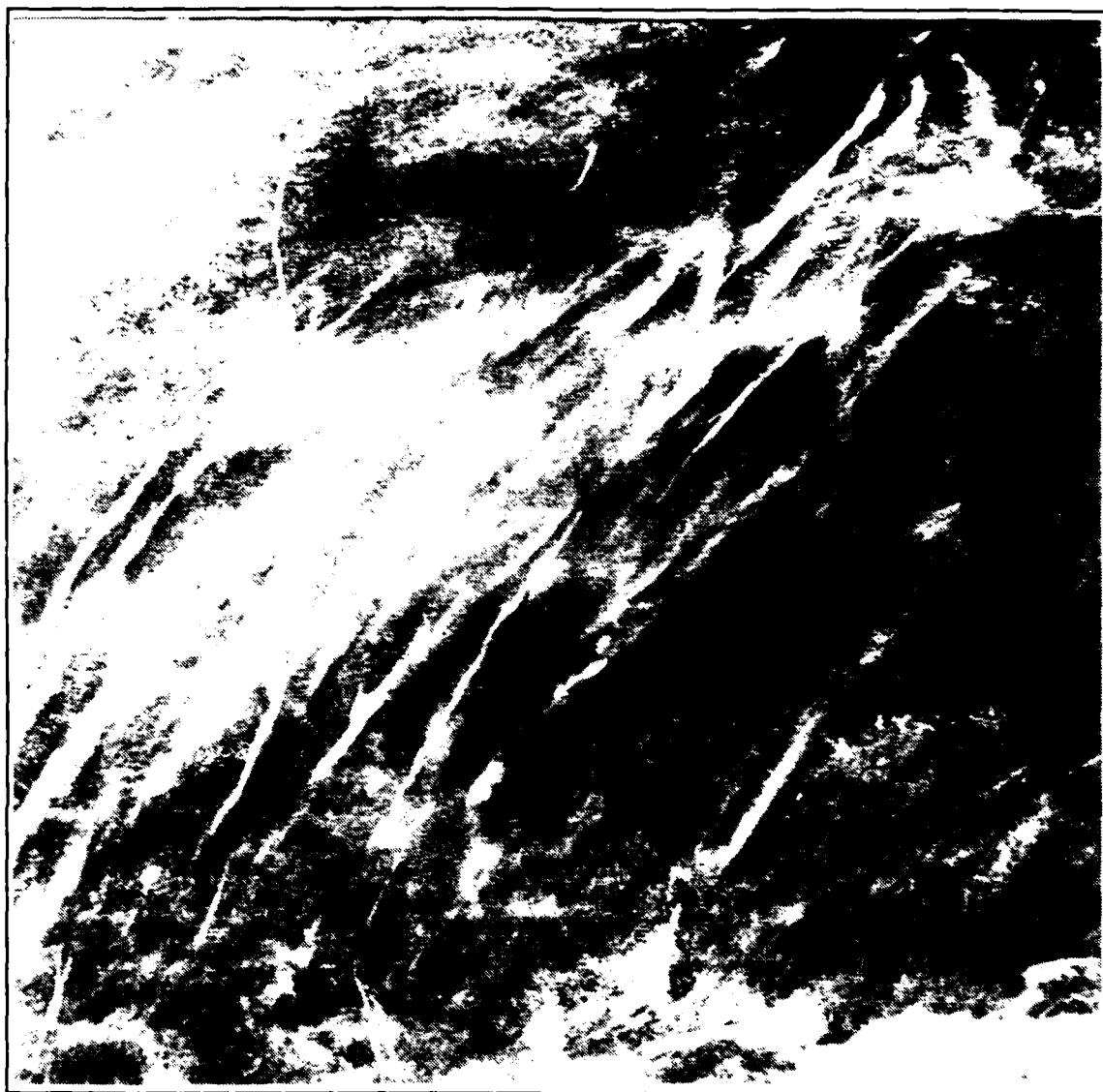


Fig. 14. Brightness temperature difference image for subscene in Fig. 12.

K. These features are suspected to be contrails. Lee (1989) was also able to identify contrails on the brightness temperature difference image. This technique could prove useful to improve contrail detection for military use. Contrail analysis also would be helpful for studies examining the contribution of contrails to high-level cloudiness.

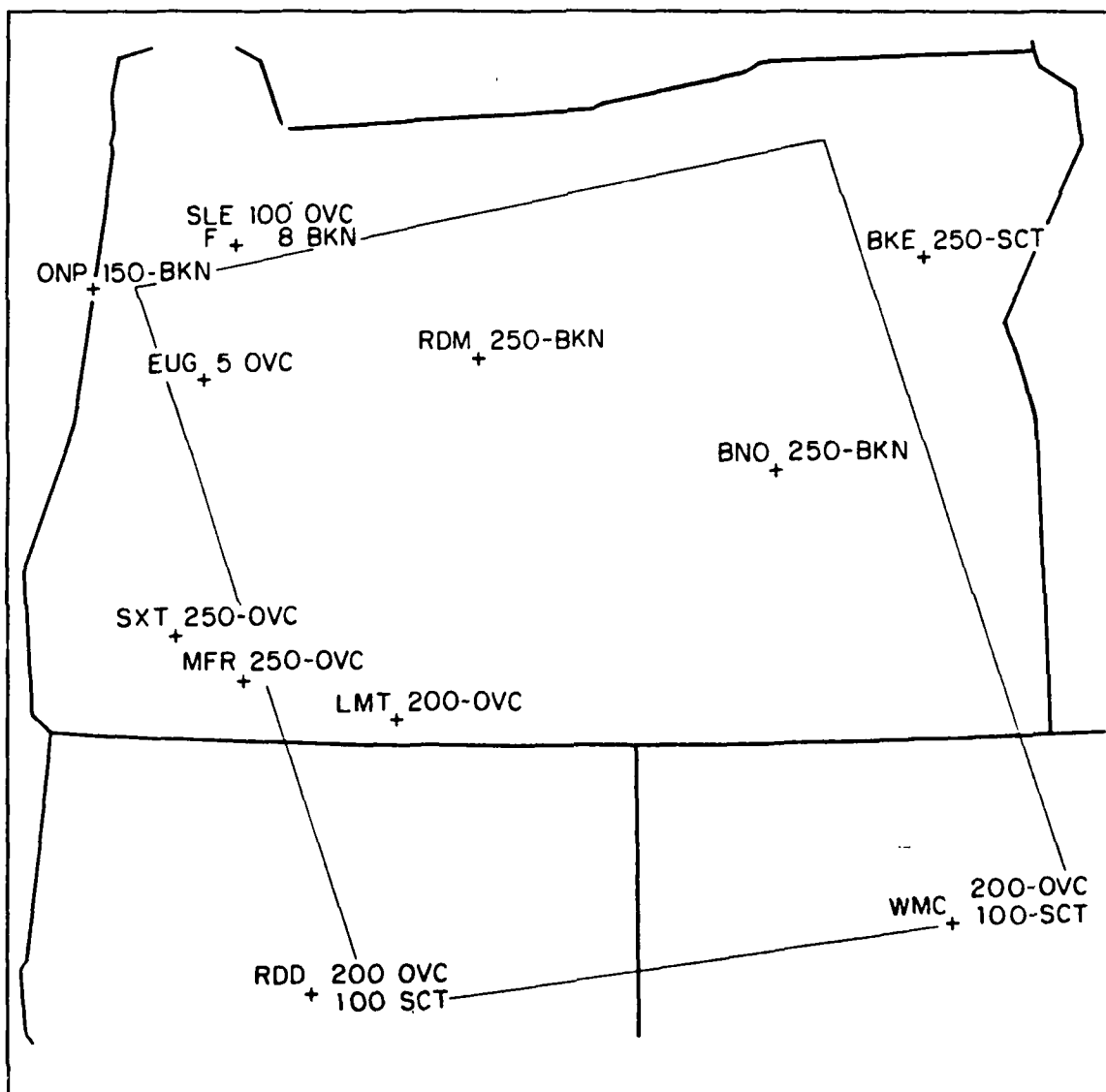


Fig. 15. Surface observations at 2300 UTC 17 January 1988 for subscene in Fig. 12.

V. RESULTS

The comparison of surface observations with BTD statistics is now presented. The basic objective is to determine if observed differences among the cloud group satellite statistics are attributed to actual differences among the BTD of the different cloud categories or to chance. The five cloud categories listed in Chapter III must have different average values in order to estimate useful thresholds. If all the categories have the same average BTD, the split-window technique cannot be used to differentiate different cloud categories.

Table 1 lists the mean, standard deviation and number of observations for the five cloud groups collected from the summer cases. For a graphical display of the BTD data a box plot for the five cloud groups is also shown in Fig. 16. The top of Table 1. **CHANNEL 4-5 DIFFERENCE STATISTICS FOR FIVE CLOUD GROUPS--SUMMER CASES.**

	PRED HI	PRED HI SCT	HI & MID	MULTI-LYR	PRECIP
MEAN	2.169	2.271	1.106	0.710	0.537
STD DEV	2.086	1.295	0.707	0.292	0.233
OBS	16	38	18	10	8

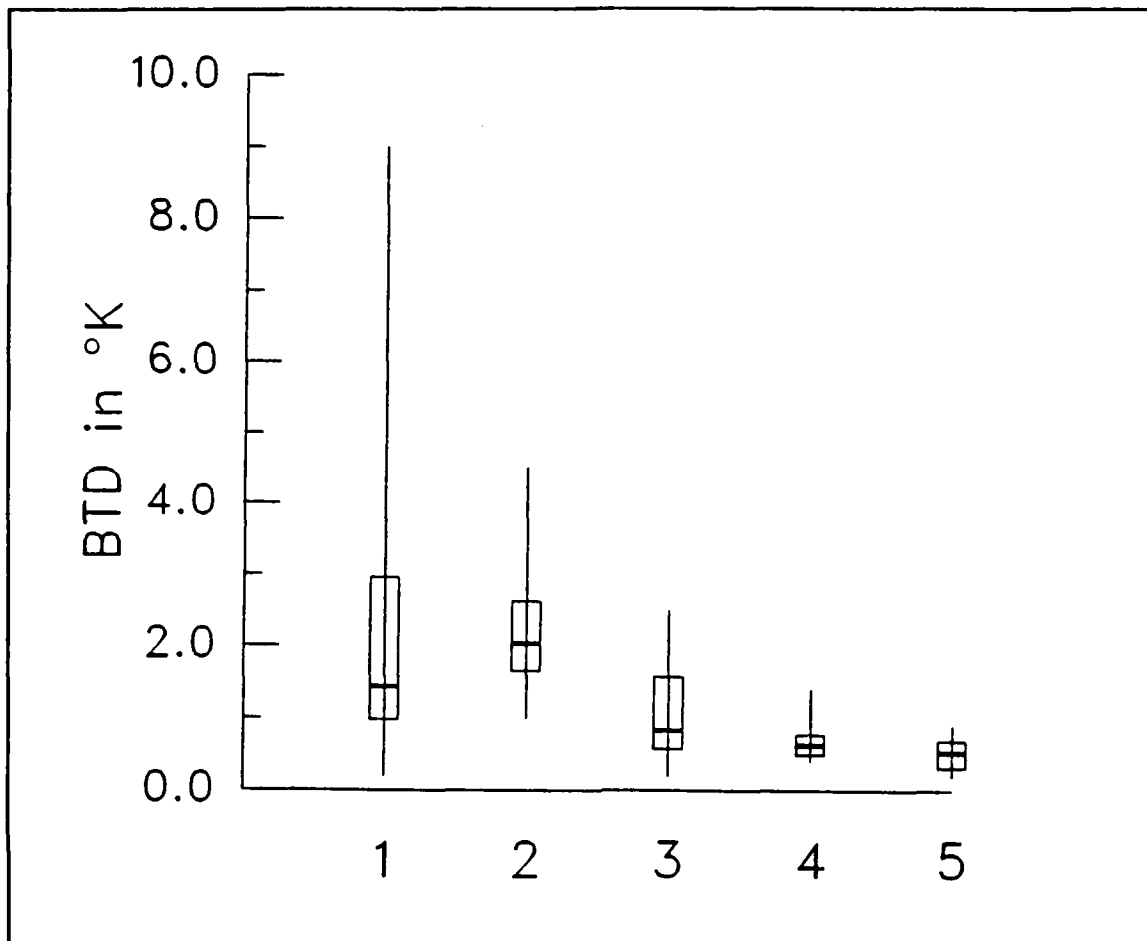


Fig. 16. Box plot of BTD data from the summer season. The five cloud groups are (1) high-level BKN or OVC, (2) high-level SCT, (3) high- and mid-level BKN or OVC, (4) multiple layered clouds and (5) stations reporting precipitation.

the line represents the 95% percentile while the bottom of the line represents the 5% percentile. The top and bottom of the box represents the 75% and 25% percentile, respectively. Finally, the line through the box represents the median.

In the summer data, it is difficult to discern differences that would allow the categorization of five cloud groups from BTD thresholds. The means (Table 1) for the first two cloud groups, predominantly high-level broken or overcast clouds and predominantly high-level scattered clouds, are very similar. These two groups will

now be combined into one cloud category named thin cirrus. Groups four (multiple layered clouds) and five (stations reporting precipitation) also are similar (Table 1 and Fig. 16). These two groups also are combined into one category named multiple layered clouds. The third group, predominantly high-level and mid-level broken or overcast clouds, was named thick cirrus or thick upper level clouds.

The statistics were recalculated for these new three cloud groups (Table 2).

Table 2. CHANNEL 4-5 DIFFERENCE STATISTICS FOR THREE CLOUD GROUPS--SUMMER CASES.

	THIN CIRRUS	THICK CIRRUS	MULTI-LAYERED
MEAN	2.241	1.106	0.633
STD DEV	1.550	0.707	0.274
OBS	54	18	18

Fig. 17 presents a box plot for the BTD data for the three cloud groups. The labels "THN", "THK" and "MUL" represent thin cirrus, thick cirrus and multiple layered clouds. An inspection of Fig. 17 suggests the thin cirrus group is clearly separate from the other two. The thick cirrus and multiple layered cloud groups are closer together.

In order to test whether the observed differences in group means is statistically significant, the F-test is employed (Dougherty 1990). The F-test is used to test the

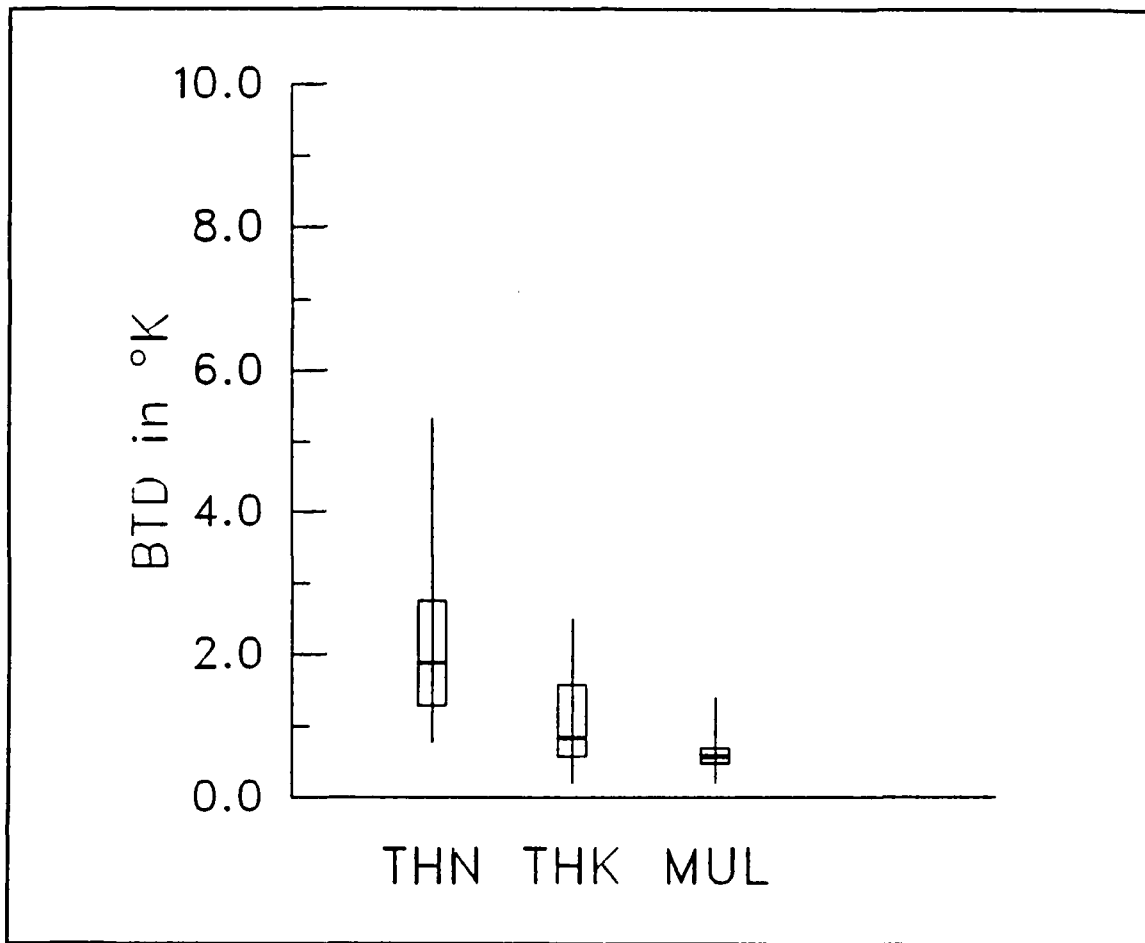


Fig. 17. Box plot of BTD data from the summer season. "THN", "THK" and "MUL" represent thin cirrus, thick cirrus and multiple layered clouds.

assumption that the cloud group means are the same, i.e. the null hypothesis: $\bar{x}_1 = \bar{x}_2 = \dots = \bar{x}_5$. The null hypothesis is not rejected if the differences among the cloud group means are small. The F-test indicates when the differences between means is sufficiently small so that any differences can be attributed to random error. The F-test uses the formula

$$F = \frac{SS_B}{SS_W}, \quad (2)$$

where

$$SS_B = \sum n_j (\bar{x}_j - \bar{x})^2 \quad (3)$$

and

$$SS_W = \sum \sum (x_i - \bar{x}_j)^2, \quad (4)$$

and n_j is the number of cloud groups, \bar{x}_j is the cloud group mean, \bar{x} is the overall mean and x_i is the individual observations within a group. SS_B reflects the variation in brightness temperature differences (BTD) attributed to population differences between groups. SS_W is attributed to random variation or noise in the BTDs within a group.

An analysis of variance is performed to express a measure of the total variation of the set of data as a sum of terms, which can be attributed to specific sources of variation. Two such sources would be (1) actual differences in the BTD of the cloud groups and (2) chance or experimental error. Table 3 lists the analysis of variance for the three cloud groups of the summer cases. The first column gives the source of the variation, DOF is the degrees of freedom, MSE is the mean square error, F is the F value calculated for the stated degrees of freedom and P is the tail probability. The tail probability gives the level of significance consistent with the presented data.

Table 3. ANALYSIS OF VARIANCE FOR THREE CLOUD GROUPS--SUMMER CASES.

SOURCE	DOF	MSE	F	P
Group	2	21.3123	13.52	0.0000
Error	87	1.5768		

The 0.01 level of significance for the F value between 2 and 80 degrees of freedom is 4.88. The F value calculated for 2 and 87 degrees of freedom from the summer data is 13.52 which exceeds 4.88. Thus, the null hypothesis can be rejected at a 0.01 level of significance. By rejecting the null hypothesis, the statement can be made that at least one of the average values of the three cloud groups is statistically different.

Tukey's test is a multiple comparison test designed to draw more specific conclusions. The technique involves the construction of simultaneous confidence intervals for the mean differences. In testing pairwise mean-equality, whenever the confidence interval for the mean differences does not contain 0, then it can be concluded that the means differ at the significance level used. (Dougherty 1990)

Table 4 lists the results of Tukey's test applied to the three cloud groups of the summer cases. The type gives the type of comparison, lower CI and upper CI refer to simultaneous lower and upper confidence interval, respectively, and difference gives the difference between the means. Comparisons significant at the 0.05 level are

indicated by "****" in the result column. The confidence intervals for the comparisons between groups 1 and 2 and between groups 1 and 3 do not contain 0. Therefore, it can be concluded that the means differ at the 0.05 significance level. The confidence interval for the comparison between groups 2 and 3 does include 0. Therefore, the means do not differ at the 0.05 significance level.

Table 4. TUKEY'S TEST RESULT FOR THREE CLOUD GROUPS--SUMMER CASES.

TYPE	LOWER CI	DIFFERENCE	UPPER CI	RESULT
1 - 2	0.3203	1.1352	1.9501	***
1 - 3	0.7925	1.6074	2.4223	***
2 - 3	-0.5258	0.4722	1.4703	

Tukey's test is a very conservative statistical test applied to several sets of data. The *t* test is an exploratory test applied to determine if the means from two data sets are statistically different. Table 5 lists the results from the *t* test applied to groups 2 and 3 of the summer cases (thick cirrus and multiple layered clouds). Type gives the group number, N is the number of observations in the group, T gives the *t* result calculated, DF is the degrees of freedom and PROB is the probability that the result is greater than *t*.

Table 5. T TEST FOR GROUPS 2 AND 3--SUMMER CASES.

TYPE	N	VARIANCES	T	DF	PROB
2	18	Unequal	2.6401	22.0	0.0149
3	18	Equal	2.6401	34.0	0.0124

The t result for 22 degrees of freedom at the 0.01 level of significance is 2.508, which is less than 2.6401, the figure calculated for the data from group 2. The t result for 30 degrees of freedom at the 0.01 level of significance is 2.457, which is less than 2.6401. Therefore, the t test gives evidence that the means for groups 2 and 3 are statistically different at a high degree of significance.

The same statistics were completed for the winter cases. Table 6 gives the summary statistics for the five cloud groups while Fig. 18 contains the box plots.

Table 6. CHANNEL 4-5 DIFFERENCES STATISTICS FOR FIVE CLOUD GROUPS--WINTER CASES.

	PRED HI	PRED HI SCT	HI & MID	MULTI-LYR	PRECIP
MEAN	1.464	1.362	1.540	1.133	1.117
STD DEV	0.787	0.880	0.635	0.058	0.183
OBS	22	8	5	3	6

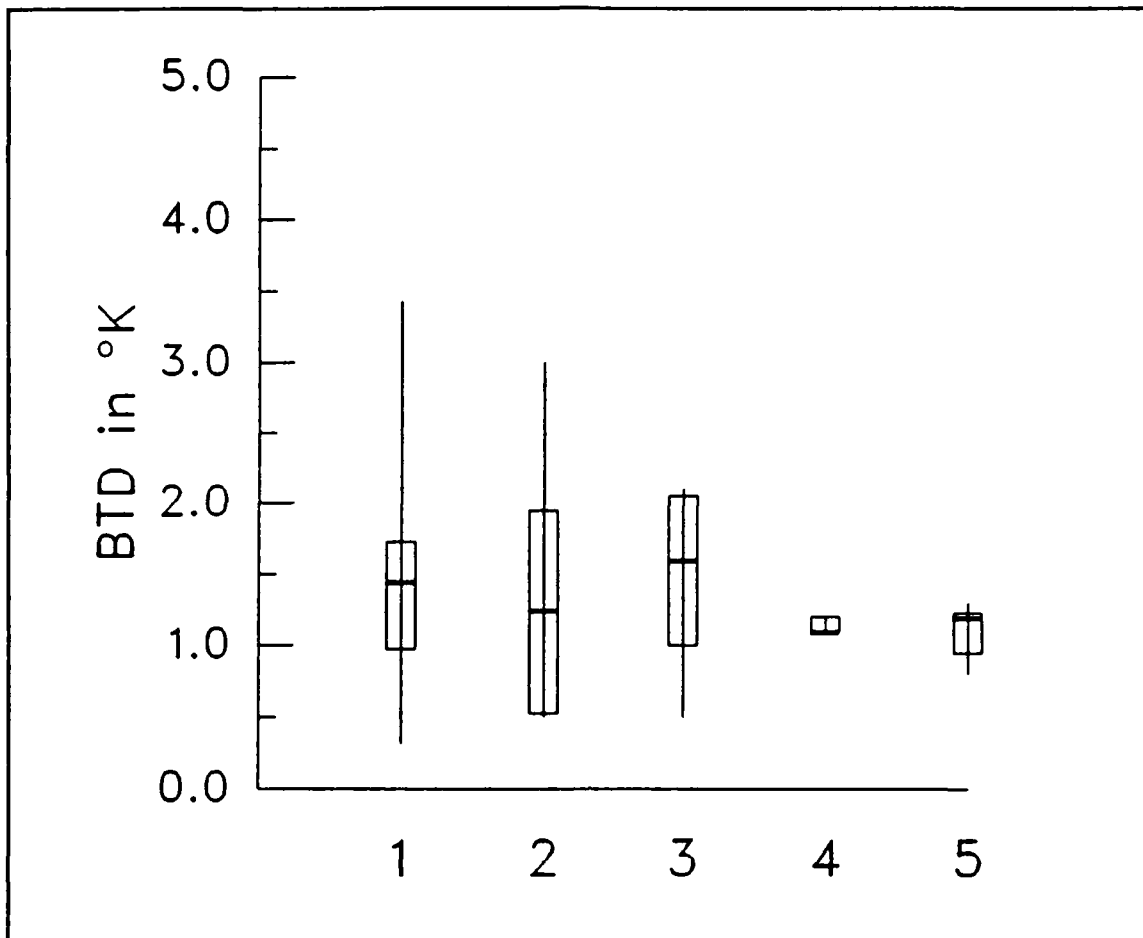


Fig. 18. Box plot of BTD data from the winter season. The five cloud groups are (1) high-level BKN or OVC, (2) high-level SCT, (3) high- and mid-level BKN or OVC, (4) multiple layered clouds and (5) stations reporting precipitation.

The data from the five cloud groups show no clear distinction between the groups. The first two cloud groups are now combined into a thin cirrus category and the last two cloud groups are combined into a multiple layered category as before. Tables 7 and 8 list the statistics and analysis of variance for these three new cloud groups for the winter cases while Fig. 19 is the box plot for the three groups of BTB data.

Table 7. STATISTICS FOR THREE CLOUD GROUPS--WINTER CASES.

	THIN CIRRUS	THICK CIRRUS	MULTI-LAYERED
MEAN	1.437	1.540	1.122
STD DEV	0.798	0.635	0.148
OBS	30	5	9

Table 8. ANALYSIS OF VARIANCE FOR THREE CLOUD GROUPS--WINTER CASES.

SOURCE	DOF	MSE	F	P
Group	2	0.4108	0.83	0.4430
Error	41	0.4946		

It is shown in Table 7 and Fig. 19 that the means of the data groups do not differ by a large margin. The F value at 0.05 level of significance for 2 and 40 degrees of freedom is 3.23. The F value at 0.4430 level of significance calculated for 2 and 41 is 0.83 (Table 8). Since $F = 0.83 < 3.23$, the null hypothesis must be accepted. The average brightness temperature differences of the groups are not statistically different.

This analysis has shown that the average brightness temperature differences for the basic three cloud groups differ for the summer cases but not for the winter cases.

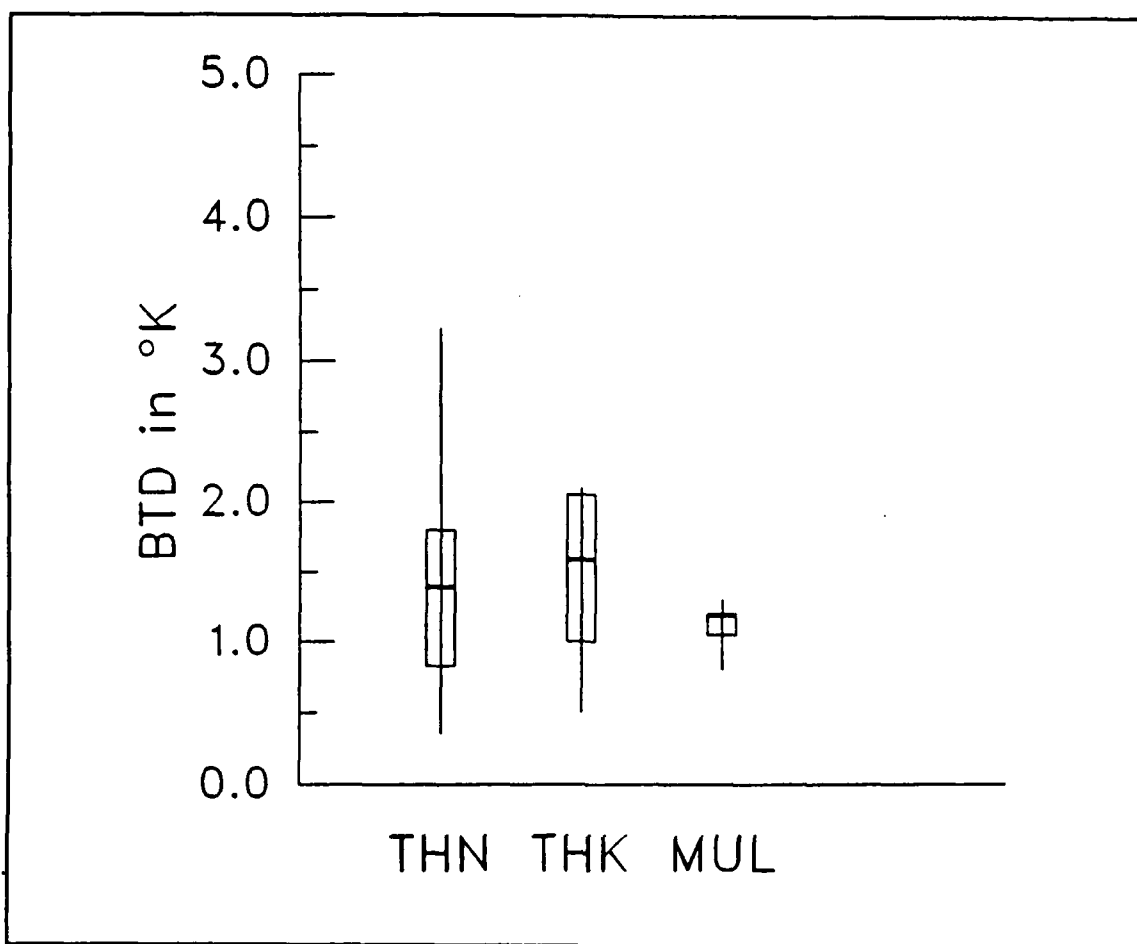


Fig. 19. Box plot of BTD data from the winter season. "THN", "THK" and "MUL" represent thin cirrus, thick cirrus and multiple layered clouds.

The surface radiance that penetrates the thin cirrus is a key factor in producing the brightness temperature differences in channel 4 versus channel 5. In the winter with cold surface temperatures, the upwelled surface radiance is significantly less than in the summer. Consequently, the BTD values are not large enough to allow classification of thin cirrus. Therefore, the split-window technique is not useful in determining brightness temperature differences for the cold season.

This technique is useful to determine the varying cirrus thicknesses during summer. The surface temperature was usually below 285 K in the cases when the technique was not successful while the surface temperature was always greater than 285 K in the successful cases. Thresholds were estimated for the three cloud groups for the summer cases by using a range near the mean for that cloud group. The BTd thresholds are given in Table 9. These thresholds are suggested to classify cirrus and multiple layered cloud analysis from this data set.

Table 9. BTd THRESHOLDS.

CLOUD GROUP	BTd THRESHOLD
Multiple Layered Clouds	0.00 to 0.80
Thick Cirrus	0.81 to 1.50
Thin Cirrus	1.51 and Greater

VI. CONCLUSIONS

This thesis studied the problem of identifying cirrus clouds in multiple channel satellite imagery. Following the work of Inoue (1985, 1987) and others, the split-window technique was applied to improve the analysis of cirrus. Cases for this study were selected over land so surface observations could be used to evaluate the use of this technique. The cases examined were all in the mid-latitudes.

Ten subscenes with areas of thick and thin cirrus, and multiple layered clouds were analyzed. The average BTD coincident with surface observations were grouped into five cloud classification groups. These groups were:

1. Predominantly high-level broken or overcast clouds, including thin overcast and thin broken.
2. Predominantly high-level scattered clouds, including thin scattered.
3. Predominantly high- and mid-level broken or overcast clouds.
4. Predominantly multiple layered clouds (high- and mid-level broken or overcast).
5. Stations reporting precipitation.

The cases were also separated for the summer and winter cases.

The BTD images were successful at distinguishing the different cloud categories. Areas of thin cirrus that were not readily visible on either the visible or IR image were represented by light areas (BTB values of 1.51 or greater) on the BTB image. Areas of thick cirrus were a light gray (BTB values from 0.81 to 1.50)

while multiple layered clouds were very dark or black (BTD values from 0.00 to 0.80). This technique complements visible and IR imagery in satellite data analysis. In addition, an unusual case with contrails was presented showing that this technique is also useful for contrail detection in certain situations.

In the summer data, it was difficult to discern differences that would allow the categorization of five cloud groups from BTD thresholds. Groups 1 (high-level BKN or OVC) and 2 (high-level SCT) were combined into one group, and groups 4 (multiple layered clouds) and 5 (stations reporting precipitation) were grouped into another. These three new cloud groups were:

1. Multiple layered clouds (combination of groups 4 and 5).
2. Thick cirrus.
3. Thin cirrus (combination of groups 1 and 2).

The average BTDs for these three cloud groups were successfully shown to be significantly different for the summer cases. Thresholds estimated from these cases are:

1. Multiple layered clouds--0.00 to 0.80.
2. Thick cirrus--0.81 to 1.50.
3. Thin cirrus--1.51 and greater.

The split-window technique was successful in distinguishing the varying cirrus thickness when the surface temperature is warmer than 285 K. The winter groups could not be separated due to the colder background. The technique complements both IR and visible imagery for data analysis purposes. This capability provides the

digital satellite image user the ability to successfully analyze cirrus. Future NOAA satellites will continue to have the split-window channel capability as will the GOES-NEXT satellite due to be launched in 1992. New digital satellite receiver and display systems such as the Mark IVB satellite van, operated by the Department of the Air Force, and the Navy's Tactical Environmental Support System (TESS-3) should be able to apply the split-window technique. Applying a color scheme to the three thresholds would provide the user the ability to quickly identify high cloud patterns of an image.

Further study should include researching the use of this technique during the transition months of spring and fall. More cases would result in more definitive statistics. With enough data points, the data could possibly be separated into monthly thresholds. The role that atmospheric water vapor plays in the brightness temperature difference is unknown. Water vapor could be estimated with the use of sounding data or by applying the split-window technique to clear air areas. Subtracting any water vapor effects from the BTD values would lead to an improved application of the split-window technique.

LIST OF REFERENCES

- Anderson, R. K., J. P. Ashman, F. Bittner, G. R. Farr, E. W. Ferguson, V. J. Oliver, and A. H. Smith, 1969: *Application of meteorological satellite data in analysis and forecasting*. Technical Report 212. Air Weather Service, Scott Air Force Base, IL, 136 pp.
- Dougherty, E. R., 1990: *Probability and statistics for the engineering, computing, and physical sciences*. Prentice Hall, Englewood Cliffs, NJ, 800 pp.
- Hunt, G. E., 1973: Radiative properties of terrestrial clouds at visible and infrared thermal window wavelengths. *Quart. J. R. Met Soc.*, **99**, 346-369.
- Huschke, R. E., 1959: *Glossary of meteorology*. American Meteorological Society, Boston, MA, 638 pp.
- Inoue, T., 1985: On the temperature and effective emissivity determination of semi-transparent cirrus clouds by bi-spectral measurements in the 10 micron window region. *J. Meteor. Soc. Japan*, **63**, 88-98.
- , 1987: A cloud type classification with NOAA-7 split-window measurements. *J. Geophys. Res.*, **92**, 3991-3999.
- Irvine, W. M., and J. B. Pollack, 1968: Infrared optical properties of water and ice spheres. *Icarus*, **8**, 324-366.
- Lee, T. F., 1989: Jet contrail identification using the AVHRR infrared split window. *J. Appl. Meteor.*, **28**, 993-995.
- Liou, K. N., 1974: On the radiative properties of cirrus in the window region and their influence on remote sensing of the atmosphere. *J. Atmos. Sci.*, **31**, 522-532.
- Platt, C. M. R., 1983: On the bispectral method for cloud parameter determination from satellite VISSR data: separating broken cloud and semitransparent cloud. *J. Clim. and Appl. Meteor.*, **22**, 429-439.

- Prabhakara, C., R. S. Fraser, G. Dalu, M. C. Wu, and R. J. Curran, 1988: Thin cirrus clouds: seasonal distribution over oceans deduced from Nimbus-4 IRIS. *J. Appl. Meteor.*, **27**, 379-399.
- Reynolds, D. W., M. L. Brown, E. A. Smith, and T. H. Vonder Haar, 1978: Cloud type separation by spectral differencing of image pairs. *Mon. Wea. Rev.*, **106**, 1214-1218.
- Schowengerdt, R. A., 1983: *Techniques for image processing and classification in remote sensing*. Academic Press, Inc., Orlando, FL, 249 pp.

INITIAL DISTRIBUTION LIST

	No. Copies
1. Defense Technical Information Center Cameron Station Alexandria, VA 22314-6145	2
2. Library, Code 0142 Naval Postgraduate School Monterey, CA 93943-5002	2
3. Commander Naval Oceanography Command Stennis Space Center, MS 39539-5000	1
4. Commanding Officer Fleet Numerical Oceanography Center Monterey, CA 93943-5005	1
5. Commanding Officer Air Force Global Weather Center Offutt Air Force Base, NE 68113-5000	1
6. Commanding Officer Naval Oceanographic and Atmospheric Research Laboratory Monterey, CA 93943-5006	1
7. Chairman (Code MR) Department of Meteorology Naval Postgraduate School Monterey, CA 93943-5000	1
8. USAFETAC/LD Air Weather Service Technical Library Scott Air Force Base, IL 62225-5000	1
9. Capt Sharon A. Wieman Det 16, 25WS Nellis AFB, NV 89191-5000	3

- | | | |
|-----|--|---|
| 10. | Prof. Carlyle H. Wash (Code MR/Wx)
Department of Meteorology
Naval Postgraduate School
Monterey, CA 93943-5000 | 8 |
| 11. | Prof. Philip A. Durkee (Code MR/De)
Department of Meteorology
Naval Postgraduate School
Monterey, CA 93943-5000 | 1 |
| 12. | Mr. Craig Motell (Code MR/MI)
Department of Meteorology
Naval Postgraduate School
Monterey, CA 93943-5000 | 1 |
| 13. | Mr. Thomas Lee
Naval Oceanographic and Atmospheric Research Laboratory
Monterey, CA 93943-5006 | 1 |
| 14. | Capt Robert C. Allen, Jr.
HQ AFSC/XTSS
Andrews AFB, DC 20334-5000 | 1 |
| 15. | AFIT/CIR
Wright-Patterson AFB, OH 45433-5000 | 1 |
| 16. | Commander
Air Weather Service
Scott Air Force Base, IL 62225-5000 | 1 |
| 17. | LtCol James R. Avant, Jr.
AFGWC/RM
Offutt Air Force Base, NE 68113-5000 | 1 |